Evaluation of Nuclear Power as a Proposed Solution to Global Warming, Air Pollution, and Energy Security

In

100% Clean, Renewable Energy and Storage for Everything

Textbook in press, *Cambridge University Press*

https://web.stanford.edu/group/efmh/jacobson/WWSBook/WWSBook.html

Mark Z. Jacobson

December 22, 2019

Contact: Jacobson@stanford.edu; Twitter @mzjacobson

Summary

In evaluating solutions to global warming, air pollution, and energy security, two important questions arise are (1) should new nuclear plants be built to help solve these problems, and (2) should existing, aged nuclear plants be kept open as long as possible to help solve these problems? To answer these questions, the main risks associated with nuclear power are examined.

The risks associated with nuclear power can be broken down into two categories: (1) risks affecting its ability to reduce global warming and air pollution and (2) risks affecting its ability to provide energy and environmental (aside from climate and air pollution) security. Risks in the former category include delays between planning and operation, emissions contributing to global warming and outdoor air pollution, and costs. Risks in the latter category include weapons proliferation risk, reactor meltdown risk, radioactive waste risk, and mining cancer and land despoilment risks. These risks are discussed, in this section. Here are additional specific findings:

- New nuclear power plants cost 2.3 to 7.4 times those of onshore wind or utility solar PV per kWh, take 5 to 17 years longer between planning and operation, and produce 9 to 37 times the emissions per kWh as wind.

- As such, a fixed amount of money spent on a new nuclear plant means much less power generation, a much longer wait for power, and a much greater emission rate than the same money spent on WWS technologies.

- There is no such thing as a zero- or close-to-zero emission nuclear power plant. Even existing plants emit due to the continuous mining and refining of uranium needed for the plant. However, all plants also emit 4.4 g-CO_2e/kWh from the water vapor and heat they release. This contrasts with solar panels and wind turbines, which reduce heat or water vapor fluxes to the air by about 2.2 g-CO_2e/kWh for a net difference from this factor alone of 6.6 g-CO_2e/kWh.

- On top of that, because all nuclear reactors take 10-19 years or more between planning and operation vs. 2-5 year for utility solar or wind, nuclear causes another 64-102 g-CO_2/kWh over 100 years to be emitted from the background grid while consumers wait for it to come online or be refurbished, relative to wind or solar.

- Overall, emissions from new nuclear are 78 to 178 g-CO_2/kWh, not close to 0.

- China's investment in nuclear plants that take so long between planning and operation instead of wind or solar resulted in China's CO_2 emissions increasing 1.3 percent from 2016 to 2017 rather than declining by an estimated average of 3 percent. The resulting difference in air pollution emissions may have caused 82,000 additional air pollution deaths in China in 2016 alone, with additional deaths in years prior and since.

Table 3.5. Total 100-year CO_2e emissions from several different energy technologies. The total includes lifecycle emissions, opportunity cost emissions, anthropogenic heat and water vapor emissions, weapons and leakage risk emissions, and emissions from loss of carbon storage in land and vegetation. All units are g-CO_2e/kWh-electricity, except the last, column, which gives the ratio of total emissions of a technology to the emissions from onshore wind. CCS/U is carbon capture and storage or use.

Technology	[a]Lifecycle emissions	[b]Opportunity cost emissions due to delays	[c]Anthropogenic heat emissions	[d]Anthropogenic water vapor emissions	[e]Nuclear Weapons risk or 100-Year CCS/U leakage risk	[f]Loss of CO_2 due to covering land or clearing vegetation	**[g]Total 100-year CO_2e**	**Ratio of 100-year CO_2e to that of wind-onshore**
Solar PV-rooftop	15-34	-12 to -16	-2.2	0	0	0	**0.8-15.8**	**0.1-3.3**
Solar PV-utility	10-29	0	-2.2	0	0	0.054-0.11	**7.85-26.9**	**0.91-5.6**
CSP	8.5-24.3	0	-2.2	0 to 2.8	0	0.13-0.34	**6.43-25.2**	**0.75-5.3**
Wind-onshore	7.0-10.8	0	-1.7 to -0.7	-0.5 to -1.5	0	0.0002-0.0004	**4.8-8.6**	**1**
Wind-offshore	9-17	0	-1.7 to -0.7	-0.5 to -1.5	0	0	**6.8-14.8**	**0.79-3.1**
Geothermal	15.1-55	14-21	0	0 to 2.8	0	0.088-0.093	**29-79**	**3.4-16**
Hydroelectric	17-22	41-61	0	2.7 to 26	0	0	**61-109**	**7.1-22.7**
Wave	21.7	4-16	0	0	0	0	**26-38**	**3.0-7.9**
Tidal	10-20	4-16	0	0	0	0	**14-36**	**1.6-7.5**
Nuclear	9-70	64-102	1.6	2.8	0-1.4	0.17-0.28	**78-178**	**9.0-37**
Biomass	43-1,730	36-51	3.4	3.2	0	0.09-0.5	**86-1,788**	**10-373**
Natural gas-CCS/U	179-405	46-62	0.61	3.7	0.36-8.6	0.41-0.69	**230-481**	**27-100**
Coal-CCS/U	230-935	46-62	1.5	3.6	0.36-8.6	0.41-0.69	**282-1,011**	**33-211**

[a]Lifecycle emissions are 100-year carbon equivalent (CO_2e) emissions that result from the construction, operation, and decommissioning of a plant. They are determined as follows:

Solar PV-rooftop: The range is assumed to be the same as the solar PV-utility range, but with 5 g-CO_2/kWh added to both the low and high ends to account for the use of fixed tilt for all rooftop PV versus the use of some tracking for utility PV.

Solar PV-utility: The range is derived from Fthenakis and Raugei (2017). It is inclusive of the 17 g-CO_2/kWh mean for CdTe panels at 11 percent efficiency, the 27 g-CO_2e/kWh mean for multi-crystalline silicon panels at 13.2 percent efficiency, and the 29 gCO_2e/kWh mean for mono-crystalline silicon panels at 14 percent efficiency. The upper limit of the range is held at the mean for multi-crystalline silicon since panel efficiencies are now much higher than 13.2 percent. The lower limit is calculated by scaling the CdTe mean to 18.5 percent efficiency, its maximum in 2018.

CSP: The lower limit CSP lifecycle emission rate is from Jacobson (2009). The upper limit is from Ko et al. (2018).

Wind-onshore and wind-offshore: The range is derived from Kaldelis and Apostolou (2017).

Geothermal: The range is from Jacobson (2009) and consistent with the review of Tomasini-Montenegro et al. (2017).

Hydroelectric and wave: From Jacobson (2009).

Tidal: From Douglass et al. (2008).

Nuclear: The range of 9-70 g-CO_2e/kWh is from Jacobson (2009), which is within the Intergovernmental Panel on Climate Change (IPCC)'s range of 4-110 g-CO_2e/kWh (Bruckner et al., 2014), and conservative relative to the 68 (10-130) g-CO_2e/kWh from the review of Lenzen (2008) and the 66 (1.4-288) g-CO_2e/kWh from the review of Sovacool (2008).

Biomass: The range provided is for biomass electricity generated by forestry residues (43 gCO_2e/kWh), industry residues (46), energy crops (208), agriculture residues (291), and municipal solid waste (1730) (Kadiyala et al., 2016).

Natural gas-CCS/U: The lower bound is for the CCGT with carbon capture plant from Skone (2015), also provided in Table 3.4. The upper bound is CCGT value without carbon capture, 506 g-CO_2e/kWh from Table 3.4, multiplied by 80 percent, which is the percent of CO_2e emissions expected to be captured from the Petra Nova facility that will remain in the air over 100 years (Table 3.6).

Coal-CCS/U: The lower bound is for IGCC with carbon capture from Skone (2015). The upper bound is the coal value without carbon capture, 1,168 g-CO_2e/kWh from Table 3.6, multiplied by 80 percent, which is the percent of coal lifecycle CO_2e emissions from the Petra Nova facility that will remain in the air over 100 years (Table 3.6).

[b]Opportunity cost emissions are emissions per kWh over 100 years from the background electric power grid, calculated from Equations 3.1 and 3.2 due to (a) the longer time lag between planning and operation of one energy technology relative to another and (b) additional downtime to refurbish a technology at the end of its useful life

compared with the other technology. The planning-to-operation times of the technologies in this table are 0.5-2 years for solar PV-rooftop; 2-5 years for solar PV-utility, CSP, wind-onshore, wind-offshore, tidal, and wave; 3-6 years for geothermal; 8-16 years for hydroelectric; 10-19 years for nuclear; 4-9 years for biomass (without CCS/U), and 6-11 years for natural gas-CCS/U and coal-CCS/U (Jacobson, 2009, except rooftop PV and natural gas-CCS/U values are added and solar PV-rooftop is updated here). The refurbishment times are 0.05-1 year for solar PV-rooftop; 0.25-1 year for solar-PV-utility, CSP, wind-onshore, wind-offshore, wave, and tidal; 1-2 years for geothermal and hydroelectric; 2-4 years for nuclear, and 2-3 years for biomass, coal-CCS/U, and natural gas-CCS/U. The lifetimes before refurbishment are 15 years for tidal and wave; 30 years for solar PV-rooftop, solar PV-utility, CSP, wind-onshore, wind-offshore; 30-35 years for biomass, coal-CCS/U, and natural gas-CCS/U; 30-40 years for geothermal; 40 years for nuclear; and 80 years for hydroelectric (Jacobson, 2009). The opportunity cost emissions are calculated here relative to the utility-scale technologies with the shortest time between planning and operation (solar-PV-utility, CSP, wind-onshore, and wind-offshore). The opportunity cost emissions of the latter technologies are, by definition, zero. The opportunity cost emissions of all other technologies are calculated like in Example 3.1 while assuming a background U.S. grid emission intensity equal to 557.3 g-CO_2e/kWh in 2017. This is derived from an electricity mix from EIA (2018d) and emissions, weighted by their 100-year GWPs, of CO_2, CH_4, and N_2O from mining, transporting, processing and using fossil fuels, biomass, or uranium. The reason tidal power has opportunity cost emissions although its planning-to-operation time is the same as onshore wind is the shorter lifetime of tidal turbines than wind turbines. Thus, tidal has more down time over 100 years than do other technologies. See Section 3.2.2.1. The opportunity cost emissions of offshore and onshore wind are assumed to be the same because new projects suggest offshore wind, particularly with faster assembly techniques and with floating turbines, are easier to permit and install now than a decade ago. Although natural gas plants don't take so long as coal plants between planning and operation, natural gas combined with CCS/U is assumed to take the same time as coal with CCS/U.

[c]Anthropogenic heat emissions here include the heat released to the air from combustion (for coal or natural gas) or nuclear reaction, converted to CO_2e (see Section 3.2.2.2). For solar PV and CSP, heat emissions are negative because these three technologies reduce sunlight to the surface by converting it to electricity. The lower flux to the surface cools the ground or a building below the PV panels. For wind turbines, heat emissions are negative because turbines extract energy from wind to convert it to electricity (Section 3.2.2.3 and Example 3.6). For binary geothermal plants (low end), it is assumed all heat is re-injected back into the well. For non-binary plants, it is assumed that some heat is used to evaporate water vapor (thus the anthropogenic water vapor flux is positive) but remaining heat is injected back into the well. The electricity from all electric power generation also dissipates to heat, but this is due to the consumption rather than production of power and is the same amount per kWh for all technologies so is not included in this table.

[d]Anthropogenic water vapor emissions here include the water vapor released to the air from combustion (for coal and natural gas) or from evaporation (water-cooled CSP, water-cooled geothermal, hydroelectric, nuclear natural gas, and coal), converted to CO_2e (see Section 3.2.2.3). Air-cooled CSP and geothermal plants have zero water vapor flux, representing the low end of these technologies. The high end is assumed to be the same as for nuclear, which also uses water for cooling. The low end for hydroelectric power assumes 1.75 kg-H_2O/kWh evaporated from reservoirs at mid to high latitudes (Flury and Frischknecht, 2012). The upper end is 17.0 kg-H_2O/kWh from Jacobson (2009) for lower latitude reservoirs and assumes reservoirs serve multiple purposes. For biomass, the number is based only on the water emitted from the plant due to evaporation or combustion, not water to irrigate some energy crops. Thus, the upper estimate is low. The negative water vapor flux for onshore and offshore wind is due to the reduced water evaporation caused by wind turbines (Section 3.2.2.3 and Example 3.6).

[e]Nuclear weapons risk is the risk of emissions due to nuclear weapons use resulting from weapons proliferation caused by the spread of nuclear energy. The risk ranges from zero (no use of weapons over 100 years) to 1.4 g-CO_2e/kWh (one nuclear exchange in 100 years) (Section 3.3.2.1). The 100-year CCS/U leakage risk is the estimated rate, averaged over 100 years, that CO_2 sequestered underground leaks back to the atmosphere. Section 3.2.2.4 contains a derivation. The leakage rate from natural gas-CCS/U is assumed to be the same as for coal-CCS/U.

[f]Loss of carbon, averaged over 100 years, due to covering land or clearing vegetation is the loss of carbon sequestered in soil or in vegetation due to the covering or clearing land by an energy facility; by a mine where the fuel is extracted from (in the case of fossil fuels and uranium); by roads, railways, or pipelines needed to transport the fuel; and by waste disposal sites. No loss of carbon occurs for solar PV-rooftop, wind-offshore, wave, or tidal power. In all remaining cases, except for solar PV-utility and CSP, the energy facility is assumed to replace grassland with the organic carbon content and grass content as described in the text. For solar PV-utility and CSP, it is assumed that the organic content of both the vegetation and soil are 7 percent that of grassland because (a) most all CSP and many PV arrays are located in deserts with low carbon storage and (a) most utility PV panels and CSP mirrors are elevated above the ground. For biomass, the low value assumes the source of biomass is

industry residues or contaminated wastes. The high value assumes energy crops, agricultural residues, or forestry residues. See Section 3.2.2.5.

[g]The total column is the sum of the previous six columns.

3.3. Why Nuclear Power Represents an Opportunity Cost

In evaluating solutions to global warming, air pollution, and energy security, two important questions that arise are (1) should new nuclear plants be built to help solve these problems, and (2) should existing, aged nuclear plants be kept open as long as possible to help solve these problems? To answer these questions, the main risks associated with nuclear power are first examined.

The risks associated with nuclear power can be broken down into two categories: (1) risks affecting nuclear's ability to reduce global warming and air pollution and (2) risks affecting nuclear's ability to provide energy and environmental (aside from climate and air pollution) security. Risks under Category 1 include delays between planning and operation, emissions contributing to global warming and outdoor air pollution, and costs. Risks under Category 2 include weapons proliferation risk, reactor meltdown risk, radioactive waste risk, and mining cancer and land despoilment risks. These risks are discussed, in this section.

Nuclear fission is the process by which tiny neutrons bombard and split certain fissile heavy elements, such as **uranium-235** (^{235}**U**) or **plutonium-239** (^{239}**Pu**) in a **nuclear reactor**. The 235 and 239 refer to the isotope, or number of protons plus neutrons in the nucleus of a uranium or plutonium atom, respectively. A **fissile** element is one that can be split during fission upon neutron bombardment and whose neutrons released during splitting can split other fissile atoms in a chain reaction. Fissile elements do not spontaneously release neutrons, creating a chain reaction. Instead, they require outside neutrons bombarding them, thereby initiating a chain reaction. ^{235}U is the only fissile element found in nature. ^{239}Pu is a product of **uranium-238** (^{238}**U**) capturing a free neutron in a nuclear reactor. The resulting ^{239}U decays to ^{239}Pu, a fissile element.

When a neutron approaches ^{235}U in a nuclear reactor, the neutron may be absorbed by or pass through the atom. Fast-moving neutrons have a higher probability of passing through the atom, whereas slow-moving neutrons have a higher probability of being absorbed. If the neutron is absorbed, the uranium atom's total energy is spread among the 236 protons and neutrons now present in the atom's nucleus. The nucleus is now unstable, and some of the uranium atoms fragment into two smaller elements, whereas the remaining atoms form ^{236}U. A variety of element pairs arise from fragmentation. Two of the most common are Krypton-92 (^{92}Kr) and Barium-141 (^{141}Ba). The fragmentation, with this product pair, also produces gamma rays and three free neutrons. The overall reaction is thus

$$1 \text{ neutron} + {}^{235}\text{U} \rightarrow {}^{92}\text{Kr} + {}^{141}\text{Ba} + 3 \text{ neutrons} + \text{gamma rays} \qquad (3.10)$$

The new neutrons may then collide with other ^{235}U atoms or with ^{239}Pu atoms, splitting them in a chain reaction. When the fragments and the gamma rays collide with water, the collision converts kinetic energy and electromagnetic energy, respectively, to massive amounts of heat.

In a **boiling water reactor** (**BWR**) **nuclear power plant**, the heat boils water directly. The high-pressure steam turns a turbine connected to a generator to produces electricity. The steam is then re-condensed to liquid water in a condenser, and the liquid water is returned back to the reactor core. In the condenser, heat from the steam is transferred to a separate (in an enclosed pipe) stream of cooling water that originates

from a lake, river, or the coastal ocean. The warmed water is then returned to where it originated from, warming the outdoor water body, creating thermal pollution. Other thermal power plants, such as those running on coal, oil, or gas, similarly warm water bodies.

In a **pressurized water reactor** (**PWR**) plant, the air pressure in the reactor is increased substantially, up to 155 bar (air pressure at Earth's surface is 1 bar). Because the boiling point of water increases with increasing atmospheric pressure, water in the reactor doesn't boil, even though the temperature in the reactor reaches 282 ^{o}C (at Earth's surface, water usually boils at 100 ^{o}C). The hot water in the reactor, which is radioactive, passes through a pipe and exchanges its heat with a different batch of water maintained at normal air pressure, causing the latter water to boil. The boiling water creates steam to run a steam turbine. The water batches are kept separate to ensure radioactive material in the high-pressure reactor does not pass through to the water vapor running through the steam turbine. BWR and PWR reactors are both **light water reactors** (**LWRs**), which are reactors that use normal water.

Uranium in a nuclear power plant is originally stored in small ceramic pellets within a metal fuel rod, often 3.7-m long. A conventional BWR or PWR nuclear reactor will go through one rod after about six years, and the rod and remaining material in it become radioactive waste. Reactors that use rods once are referred to as **once-through** reactors. The radioactive waste in the fuel rod must be stored for several hundred thousand years.

A fuel rod that has gone through a fission reactor once still has 99 percent of its uranium left over, including slightly more ^{235}U than natural uranium. This remaining uranium and its fission product, plutonium, can be extracted and reprocessed for use in a **breeder reactor**, extending the life of a given mass of uranium and reducing waste significantly. However, the reprocessing increases both the cost and the production of ^{239}Pu by the collision of ^{238}U with fast moving neutrons. Breeder reactors can thus be optimized to produce ^{239}Pu for use in nuclear weapons (Karam, 2006), so they are a concern with respect to weapons proliferation.

As of 2019, over 400 active nuclear reactors provide electric power among 31 countries. Only two of these reactors are breeder reactors. For this number of reactors, uranium mines produce about 60,000 tonnes of uranium per year (World Nuclear Association, 2019). Uranium reserves (aside from hard-to-extract uranium in seawater) as of 2015 were about 7.6 million tonnes. This suggests that about 127 years of uranium are available for current once-through fuel cycle reactors at near-current rates of uranium use. As such, even if the issues discussed below were not issues, uranium is a limited resource, and growing nuclear power will deplete uranium faster.

An alternative fuel to uranium in nuclear reactors is thorium. **Thorium**, like uranium, can be used to produce nuclear fuel in a breeder reactor. The advantage of thorium is that it produces less long-lived radioactive waste than does uranium. Its products are also more difficult to convert into nuclear weapons material. However, thorium still produces ^{232}U, which was used in one nuclear bomb core produced during the **Operation Teapot** bomb tests in 1955. Thus, thorium is not free of nuclear weapons proliferation risk. In addition, thorium reactors require the same long time lag between planning and operation as uranium reactors (Section 3.3.1.1) and most likely longer because hardly any contractors or scientists have experience building or running thorium reactors. Thus, thorium reactors will produce greater emissions from the background electric grid compared with WWS technologies, which have a shorter time lag. Finally, lifecycle emissions of carbon from a thorium reactor are similar to those from a uranium reactor.

A proposed alternative to the large once-through reactor and the breeder reactor is the **small modular reactor (SMR)**. SMRs are nuclear fission reactors that are much smaller than a traditional reactor and prefabricated in a factory. The purpose of prefabricating much of the reactor is to reduce construction time, costs, and mistakes during construction. The reactor would then be moved to its final site, where construction would be completed. Many types of SMRs have been proposed, including miniature versions of current reactors as well as new designs.

One type of new design is a **fast reactor**, in which the fuel is reformulated to allow fast-moving neutrons, rather than slow-moving neutrons, to split an atom. One way to do this is to increase ^{239}Pu, which absorbs more fast-moving neutrons than does ^{235}U. Fast reactors can be turned into breeder reactors by surrounding the core with ^{238}U, which absorbs a fast-moving neutron to become ^{239}U, which decays to ^{239}Pu.

Whereas slow reactors still produce significant radioactive waste, fast reactors produce less waste but also increase the potential for nuclear weapons proliferation by producing more ^{239}Pu. Because slow and fast SMRs are small and modular, many countries that don't currently have nuclear energy facilities could more readily purchase them, increasing the risk of nuclear weapons proliferation. Most SMRs also have meltdown risk. They also require uranium. Slow reactors have the same resource limitation, lung cancer risk, and land despoilment risk associated with uranium mining as do non-SMRs (Section 3.3.2.4). Finally, because SMRs have not been commercialized to date, their emissions, time lag between planning and operation, and cost are still not known.

Finally, **nuclear fusion** of light atomic nuclei (e.g., protium, deuterium, or tritium) could theoretically supply power indefinitely without long-lived radioactive waste because the products are isotopes of helium. However, little prospect exists for fusion to be commercially available for at least 50 to 100 years, if ever.

Nuclear power from fission first became a source of electric power in the 1950s. The first nuclear power plant to produce electricity was an experimental reactor in Arco, Idaho. On December 20, 1951, it powered four light bulbs. On June 26, 1954, a 5 MW nuclear reactor was connected to the electric power grid for industrial use in Obninsk, Russia. Subsequently, on August 27, 1956, a 50 MW reactor was connected to the grid for commercial use in Windscale, England.

Below, the risks associated with nuclear power are discussed in detail.

3.3.1. Risks Affecting the Ability of Nuclear Power to Address Global Warming and Air Pollution

The first category of risk associated with nuclear power includes risks affecting nuclear power's ability to reduce global warming and air pollution. These risks include the long lag times between planning and operating and to refurbish a nuclear reactor, nuclear's high carbon equivalent emissions relative to WWS technologies, and nuclear's high cost.

3.3.1.1. Delays Between Planning and Operation and due to Refurbishing Reactors

The longer the time lag between the planning and operation of an energy facility, the more the air pollution and climate-relevant emissions from the background electric power grid (Section 3.2.2). Similarly, the longer the time required to refurbish a plant for continued use at the end of its life, the greater the emissions from the background grid while the plant is down.

The time lag between planning and operation of a nuclear power plant includes the times to obtain a construction site, a construction permit, an operating permit, financing, and insurance; the time between construction permit approval and issue; and the construction time of the plant.

In March 2007, the United States Nuclear Regulatory Commission approved the first request for a site permit in 30 years. This process took 3.5 years. The time to review and approve a construction permit is another 2 years and the time between the construction permit approval and issue is about 0.5 years. Thus, the minimum time for preconstruction approvals (and financing) in the United States is 6 years. An estimated maximum time is 10 years. The time to construct a nuclear reactor depends significantly on regulatory requirements and costs. Although nuclear reactor **construction times** worldwide are often shorter than the 9-year median construction times in the United States since 1970 (Koomey and Hultman, 2007), they averaged 7.4 years worldwide in 2015 (Berthelemy and Rangel, 2015). As such, a reasonable estimated range for construction time is 4 to 9 years, bringing the overall time between planning and operation of a nuclear power plant worldwide to 10 to 19 years.

An examination of some recent nuclear plant developments confirms that this range is not only reasonable, but an underestimate in at least one case. The **Olkiluoto 3** reactor in Finland was proposed to the Finnish cabinet in December 2000 to be added to an existing nuclear power plant. Its latest estimated completion date is 2020, giving a **planning-to-operation** (**PTO**) time of 20 years. The **Hinkley Point** nuclear plant was planned, starting in 2008. Construction began only on December 11, 2018. It has an estimated completion year of 2025 to 2027, giving it a PTO time of 17 to 19 years. The **Vogtle 3 and 4** reactors in Georgia were first proposed in August 2006 to be added to an existing site. The anticipated completion dates are November 2021 and November 2022, respectively, given them PTO times of 15 and 16 years, respectively. Their construction times will be 8.5 and 9 years, respectively. The **Flamanville**, France, Unit 3 reactor was planned on an existing nuclear site starting in 2004. A contract was awarded in 2005. Construction started in 2007 but is not expected to be completed until 2023, for a construction time of 16 years and PTO time of 19 years. The **Haiyang 1 and 2** reactors in China were planned starting in 2005. Construction started in 2009 and 2010, respectively. Haiyang 1 began commercial operation on October 22, 2018. Haiyang 2 began operation on January 9, 2019, giving them construction times of 9 years and PTO times of 13 and 14 years, respectively. The **Taishan 1 and 2** reactors in China were bid in 2006. Construction began in 2008. Taishan 1 began commercial operation on December 13, 2018. Taishan 2 began operation on September 9, 2019, giving them construction times of 10 and 11 years and PTO times of 12 and 13 years, respectively. Planning and procurement for four reactors in **Ringhals**, Sweden started in 1965. One took 10 years, the second took 11 years, the third took 16 years, and the fourth took 18 years to complete. In sum, PTO times for both recent and historic nuclear plants have mostly been in the range of 10 to 19 years.

Some contend that France's 1974 Messmer Plan resulted in the building of its 58 reactors in 15 years. The **Messmer Plan** was a proposal, enacted without public or parliamentary debate, by the Prime Minister of France, Pierre Messmer, to build 80 nuclear reactors by 1985 and 170 by 2000. In fact, the plan had been in the works for years prior and was only proposed publicly following the international oil crisis of 1973 (Morris, 2015). For example, the Fessenheim nuclear reactor obtained its construction permit in 1967 and was planned before that. In addition, 10 of the reactors were completed only between 1991 and 2000. As such, the whole planning-to-operation time for the 58 reactors was at least 33 years, not 15. That of any individual reactor was 10 to 19 years.

Planning-to-operation delays are not the only cause of background emissions associated with nuclear power or any other energy technology. Nuclear reactors have an expected lifetime on the order of 40 years. To run longer, they need to be refurbished. An estimate of the time to refurbish a nuclear reactor is 2-4 years. Refurbishment of the Darlington 2, Ontario nuclear reactor, for example, began in October 2016 and is scheduled to take 3 years and 4 months (World Nuclear News, 2018).

Equations 3.1 and 3.2 provide an estimate of the opportunity cost CO_2e emissions resulting from emissions from the background due to a nuclear power plant's long PTO time and refurbishment time. Table 3.5 provides an overall estimate of this opportunity cost emissions as 64 to 102 g-CO_2e/kWh, which is higher than nuclear's lifecycle emissions. Opportunity cost emissions also include health-affecting air pollution emissions.

Transition highlight. Example 3.11 illustrates how China's investment in nuclear plants, which have long planning-to-operation times, instead of wind power resulted in China's CO_2 emissions rising 1.3 percent from 2016 to 2017 rather than declining by an estimated average of 3 percent during that period. A similar result would be found if China invested in solar instead of nuclear.

The health impacts of such delays in China are substantial. In 2016, 1.9 million people died of from air pollution particles and gases in China (Table 7.14). Assuming that air pollution emissions are proportional to CO_2 emissions, **82,000 (1.9 million × 4.3 percent) more people may have died in 2016 alone due to China's investment in nuclear instead of wind or solar**. Additional deaths likely occurred prior and since. Thus, opportunity-cost emissions affect both climate and health.

Example 3.11. Did construction of nuclear plants in China cause its emissions to rise between 2016 and 2017?
Between 2016 and 2017, the CO_2 emission rate in China (including Hong Kong) increased by 121 million metric tonnes (MT), or 1.3 percent, over its 2016 emission rate of 9,310 MT-CO_2 (British Petroleum, 2018). During that period, China had 14 GW of nuclear power under construction, with planning for all the plants starting before 2012. The capital cost of a new nuclear power plant ranges from $6,500/kW to $12,250/kW, whereas that of a new wind turbine ranges from $1,150/kW to $1,550/kW (Lazard, 2018). Assuming the capital for the nuclear plants had been invested in wind instead and the wind turbines had been installed prior to 2017 (because the planning to operation time of wind is 2 to 5 years versus 10 to 19 years for nuclear), estimate the 2017 CO_2 emissions that would have been avoided. Assume the wind turbine capacity factor ranges from 0.3 to 0.37 and that the CO_2 emission intensity of the grid in China is between 850 and 900 g-CO_2/kWh (Li et al., 2017).

Solution:
Dividing the high (and low) capital cost of nuclear per kW by the low (and high) capital cost of wind per kW and multiplying the result by 14 GW gives a range of 58.7 to 149 GW nameplate capacity of wind that could have been installed and running prior to 2017. Multiplying by the capacity factor range of wind and 8,760 hours per year and dividing by 1,000 GW per TW gives the annual energy output of the wind that could have been installed as 154 to 483 TWh/y. Multiplying this range by the CO_2 emission intensity that wind would have avoided, 850 to 900 g-CO_2/kWh, and by 10^9 kWh/TWh, and dividing by 10^{12} g/MT gives 131 to 435 MT-CO_2/y avoided. In other words, investing in wind instead of nuclear would have resulted in China decreasing its CO_2 emissions by about 1.4 to 4.7 percent (for an average of 3.0 percent) instead of increasing it by 1.3 percent. As such, investing in nuclear has caused an opportunity cost CO_2 emission in China.

3.3.1.2. Air Pollution and Global Warming Relevant Emissions From Nuclear

Nuclear power contributes to global warming and air pollution in the following ways: (1) emissions of air pollutants and global warming agents from the background grid due to its long planning-to-operation and refurbishment times (Section 3.2.2.1); (2) **lifecycle emissions** of air pollutants and global warming agents during construction, operation, and decommissioning of a nuclear plant; (3) heat and water vapor emissions during the operation of a nuclear plant (Sections 3.2.2.2 and 3.2.2.3); (4) carbon dioxide emissions due to covering soil or clearing vegetation during the construction of a nuclear plant, uranium mine, and waste site (Section 3.2.2.5); and (5) the emissions risk of air pollutants and global warming agents due to nuclear weapons proliferation (Section 3.3.2.1).

Every one of these categories represents an actual emission or emission risk, yet most of these emissions, except for lifecycle emissions, are incorrectly ignored in virtually all studies of nuclear energy impacts on climate. Virtually no study considers the impact of nuclear energy on air pollution mortality. By ignoring these factors, studies distort the impacts on climate and air pollution health associated with some technologies over others.

Table 3.5 summarizes the CO_2e emissions from nuclear power from each of the five categories just described. The table indicates that the opportunity cost emissions of nuclear (64 to 102 g-CO_2e/kWh) are higher than the lifecycle emissions (9 to 70 g-CO_2e/kWh). The range of lifecycle emissions estimated in Table 3.5 for nuclear power is well within the "*range of harmonized lifecycle greenhouse gas emissions reported in the literature*," 4 to 110 g-CO_2e/kWh, from the Intergovernmental Panel on Climate Change review (Bruckner et al., 2014, p. 540). It is also conservative relative to the 68 (10 to 130) g-CO_2e/kWh from the review of Lenzen (2008) and relative to the 66 (1.4 to 288) g-CO_2e/kWh from the review of Sovacool (2008).

Emissions from the heat and water vapor fluxes from nuclear (totaling 4.4 g-CO_2-kWh) alone suggest that during the life of an existing nuclear power plant, **nuclear can never be a zero-carbon-equivalent technology**, even if its lifecycle emissions from mining and refining uranium were zero. On the other hand, the emissions from nuclear due to covering and clearing soil are relatively small (0.17 to 0.28 g-CO_2e/kWh). Finally, Table 3.5 provides a low estimate (zero) and a high estimate (1.4 g-CO_2e/kWh) for the 100-year risk of CO_2e emissions associated with nuclear weapons proliferation due to nuclear energy. These numbers are derived in Section 3.3.2.1.

The total CO_2e emissions from nuclear power in Table 3.5 are 78 to 178 g-CO_2e/kWh. These emissions are 9 to 37 times the CO_2e emissions from onshore wind power. The ratio of health-affecting air pollutant emissions from nuclear relative to onshore wind is 7 to 25. This is determined by considering only the lifecycle, opportunity cost, and weapons proliferation emissions from nuclear and wind in Table 3.5.

Although the emissions from nuclear are lower than from coal or natural gas with carbon capture, nuclear power's high CO_2e emissions coupled with its long planning-to-operation time render it an opportunity cost relative to the faster-to-operate and lower-emitting alternative WWS technologies (Jacobson, 2009).

3.3.1.3. Nuclear Costs

The third risk of nuclear power related to its ability to reduce global warming and air pollution is the high cost for a new nuclear reactor relative to most WWS technologies. In addition, the cost of running existing nuclear reactors has increased significantly, and the costs of new WWS technologies have dropped so much, that many existing reactors are shutting down early due to high costs. Others have requested large subsidies to stay open. In this section, nuclear costs are discussed briefly.

The levelized cost of energy (LCOE) for a new nuclear plant in 2018, based on calculations by Lazard (2018), is $151 (112 to 189)/MWh, where $100/MWh equals 10 ¢/kWh. This compares with $43 (29 to 56)/MWh for onshore wind and $41 (36 to 46)/MWh for utility-scale solar PV from the same source (Table 7.9). A good portion of the high cost of nuclear is related to its long planning-to-operation time, which in turn is partly due to construction delays.

This nuclear LCOE is an underestimate for several reasons. First, Lazard assumes a construction time for nuclear of 5.75 years. However, the Vogtle 3 and 4 reactors, though will take at least 8.5 to 9 years to finish construction. This additional delay alone results in an estimated LCOE for nuclear of about $172 (128 to 215)/MWh, or a cost 2.3 to 7.4 times that of an onshore wind farm (or utility PV farm).

Next, the LCOE does not include the cost of the major nuclear meltdowns in history. For example, the estimated cost to clean up the damage from three Fukushima Dai-ichi nuclear reactor core meltdowns in 2011 (Section 3.3.2.2) was $460 to $640 billion (Denyer, 2019). This is equivalent to a mean of about $1.2 billion, or 10 to 18.5 percent of the capital cost, of every nuclear reactor that exists worldwide.

In addition, the LCOE does not include the cost of storing nuclear waste for hundreds of thousands of years. In the U.S. alone, about $500 million is spent yearly to safeguard nuclear waste from about 100 civilian nuclear energy plants (Garthwaite, 2018). This amount will only increase as waste continues to accumulate. After the plants retire, the spending must continue for hundreds of thousands of years with no revenue stream from electricity sales to pay for the storage.

The spiraling cost of new nuclear plants in recent years has resulted in the cancelling of several nuclear reactors under construction (e.g., two reactors in South Carolina) and in requests for subsidies to keep construction projects alive (e.g., the two Vogtle reactors in Georgia). High costs have also reduced the number of new constructions to a crawl in liberalized markets of the world. However, in some countries, such as China, nuclear reactor growth continues due to large government subsidies, albeit with a 10- to 19-year time lag between planning and operation (Section 3.3.1.1) and escalating costs.

In sum, before accounting for meltdown damage and waste storage, **a new nuclear power plant costs 2.3 to 7.4 times that of an onshore wind farm (or utility PV farm), take 5 to 17 years longer between planning and operation, and produces 9 to 37 times the emissions per unit electricity generated**. Thus, a fixed amount of money spent on a new nuclear plant means much less power generation, a much longer wait for power, and much greater emission rate than the same money spent on WWS technologies.

The Intergovernmental Panel on Climate Change similarly concluded that the economic, social, and technical feasibility of nuclear power have not improved over time,

> "*The political, economic, social and technical feasibility of solar energy, wind energy and electricity storage technologies has improved dramatically over the past few years, while that of nuclear energy and Carbon Dioxide Capture and Storage (CCS) in the electricity sector has not shown similar improvements."* (de Coninck et al., 2018, page 4-5)

Costs of existing operating nuclear plants have also escalated tremendously, forcing some plants either to shut down early or request large subsidies to stay open. Whether an existing nuclear plant should be subsidized to stay open should be evaluated on a case-by-case basis. The risk of shutting a functioning nuclear plant is that its energy may be replaced by higher-emitting fossil fuel generation. However, the risk of subsidizing the plant is that the funds could otherwise be used immediately to replace the nuclear plant with lower-cost and lower-emitting wind or solar electricity generation. Because the nuclear plant would usually need to be replaced within a decade in any case, simply incurring the cost of new renewables now will almost always be less expensive than spending the same money on renewables in ten years and paying nuclear a subsidy today.

For example, in 2016, three existing upstate New York nuclear plants requested and received subsidies to stay open using the argument that the plants were needed to keep emissions low. However, Cebulla and Jacobson (2018) found that subsidizing such plants may increase carbon emissions and costs relative to replacing the plants with wind or solar. For different nuclear plants and subsidy levels, the results could change, which is why each plant needs to be evaluated individually.

3.3.2. Risks Affecting the Ability of Nuclear Power to Address Energy and Environmental Security

The second category of risk related to nuclear power is the risk of the plant not being able to provide stable energy and environmental security. One reason for this is the risk of nuclear meltdown. Others are its risks of increasing weapons proliferation, radioactive waste exposure, and damage (cancer and land degradation) due to uranium mining. WWS technologies do not have these risks.

3.3.2.1. Weapons Proliferation Risk

The first risk of nuclear power related to energy and environmental security is weapons proliferation risk. The growth of nuclear energy has historically increased the ability of nations to obtain or harvest plutonium or enrich uranium to manufacture nuclear weapons. As stated by Fuhrmann (2009),

> "*Peaceful nuclear cooperation and nuclear weapons are related in two key respects. First, all technology and materials related to a nuclear weapons program have legitimate civilian applications. For example, uranium enrichment and plutonium reprocessing facilities are dual-use in nature because they can be used to produce fuel for power reactors or fissile material for nuclear weapons. Second, civilian nuclear cooperation builds-up a knowledge-base in nuclear matters*."

The Intergovernmental Panel on Climate Change recognizes this fact. They conclude, with "*robust evidence and high agreement*" that nuclear weapons proliferation concern is a barrier and risk to the increasing development of nuclear energy:

> "*Barriers to and risks associated with an increasing use of nuclear energy include* ***operational risks*** *and the associated safety concerns,* ***uranium mining risks****, financial and regulatory risks,* ***unresolved waste management issues, nuclear weapons proliferation concerns****, and adverse public opinion).* (Bruckner et al., 2014, Executive Summary, p. 517).

The building of a nuclear reactor for energy in a country that does not currently have a reactor increases the risk of nuclear weapons development in that country. Specifically, it allows the country to import uranium for use in the nuclear energy facility. If the country so chooses, it can secretly enrich the uranium to create weapons grade uranium as well as harvest plutonium from uranium fuel rods used in a nuclear reactor, for nuclear weapons. This does not mean any or every country will do this, but historically some have, and the risk is high, as noted by IPCC.

The next risk is whether a nuclear weapon developed in this manner is used. That risk also ranges from zero to some risk. If a weapon is used, it may kill 2 to 20 million people and burn down a megacity, releasing substantial emissions. As such, beyond the horrible risk of loss of human life, there is a risk of zero to some nonzero emission rate from nuclear weapons proliferation resulting from nuclear energy proliferation. This risk is quantified later in this section. First, the difference between weapons grade and reactor grade uranium and plutonium is described.

Uranium ore is mined in an open pit or underground and contains 0.1 to 1 percent uranium by mass. The ore is milled to concentrate the uranium in the form of a yellow power called **yellowcake**, which contains about 80 percent uranium oxide. Uranium is then processed further into uranium dioxide or uranium hexafluoride for use in nuclear reactors. However, before the uranium can be used in a reactor, it must first be enriched.

Of all uranium on Earth, 99.2745 percent is ^{238}U, 0.72 percent is ^{235}U, and 0.0055 percent is ^{234}U. Thus, less than 1 percent is ^{235}U. ^{238}U has a half-life of 4.5 billion years. Most commercial light water nuclear reactors use uranium consisting of 3 to 5 percent ^{235}U. As such, the concentration of ^{235}U in the uranium fuel rod must be increased from its ore concentration. This is done by enrichment. **Uranium enrichment** is the process of separating the isotopes of uranium to increase the percent of ^{235}U in a batch. Enriched uranium is useful for both nuclear energy and nuclear weapons.

Enrichment is done either by gas diffusion, centrifugal diffusion, or mass separation by magnetic field. Only gas diffusion and centrifugal diffusion are commercial processes, and most enrichment today is by **centrifugal diffusion** because it consumes only 2 to 2.5 percent the energy as gas diffusion. Nevertheless, centrifugal diffusion still requires many centrifuges running for long periods, thus lots of energy. Centrifugal diffusion works by spinning a cylindrical container containing uranium. The heavier ^{238}U atoms collect toward the outside edge of the cylinder and the lighter ^{235}U atoms collect toward the inside.

Uranium with less than 20 percent ^{235}U is called **low enriched uranium**. **Highly enriched uranium** contains 20 to 90 percent ^{235}U. A nuclear weapon can be made with highly enriched uranium. However, weapons increase their destructiveness with more enrichment. Thus, ninety percent or more ^{235}U is considered **weapons grade uranium** and is generally used with enriched plutonium in a nuclear bomb. An estimated 9,000 centrifuges can produce enough weapons grade ^{235}U for one nuclear weapon from natural uranium in about seven months. With 5,000 centrifuges, the process takes about one year (IranWatch, 2015). Because uranium in a fuel rod used for nuclear energy has only 3 to 5 percent ^{235}U and even less once it goes through a nuclear reactor, spent fuel rods are not considered a useful source of weapons grade uranium.

Plutonium is also used in nuclear weapons. 10 kg of ^{239}Pu was used in the bomb dropped on Nagasaki. Plutonium can be obtained from a once-through nuclear reactor running on a reactor grade uranium fuel rod. When ^{235}U decays and releases neutrons in a nuclear reactor, a neutron can bind with a ^{238}U atom to produce ^{239}U, which decays to produce ^{239}P. Plutonium that is 93 percent or more ^{239}Pu is considered weapons grade plutonium. Plutonium less than 80 percent plutonium is reactor grade. Because any plutonium can be used to make a bomb and is easier to obtain than enriching uranium (since plutonium can be harvested from a fuel rod running through a nuclear reactor), plutonium is considered the element of even greater concern than uranium with respect to nuclear weapons proliferation.

A large-scale worldwide increase in nuclear energy facilities would exacerbate the risk of nuclear weapons proliferation. In fact, producing material for a weapon requires merely operating a civilian nuclear power plant together with a sophisticated plutonium separation facility. The historic link between nuclear energy facilities and weapons is evidenced by the development or attempted development of weapons capabilities secretly under the guise of peaceful civilian nuclear energy or nuclear energy research programs in Pakistan, India, Iraq (prior to 1981), Syria (prior to 2007), Iran, and, North Korea, among other countries.

If the world's all-purpose energy were converted to electricity and electrolytic hydrogen by 2050, the ~9 trillion watts (TW) in resulting annual average end-use electric power demand would require about 12,500 850-MW nuclear reactors (31 times the number of active reactors today), or one installed every day for 34 years. Not only is this construction time impossible given the long PTO of nuclear, but it would also result in all known reserves of uranium worldwide for once-through reactors running out in about three years. As such, there is no possibility the world will run solely on once-through nuclear energy by 2050.

Even if only 6.4 percent of the world's energy were supplied with nuclear, the number of active nuclear reactors worldwide would nearly double to around 800. Many more countries would possess nuclear

reactors, increasing the risk that some of these countries would use the facilities to mask the development of nuclear weapons, as has occurred historically.

If a country were to develop a weapon as a result of its acquisition of one or more nuclear energy facilities, the risk that it would use the weapons is not zero. Here, the emissions associated with a limited nuclear exchange are quantified.

The explosion of fifty 15-kilotonne nuclear devices (a total of 1.5 megatonne, or 0.1 percent of the yield of a full-scale nuclear war) during a limited nuclear exchange in a megacity would kill 2.6 to 16.7 million people from the explosion and burn 63 to 313 Tg of city infrastructure, adding 1 to 5 Tg of warming and cooling aerosol particles to the atmosphere, including much of it to the stratosphere (Jacobson, 2009). The particle emissions would cause significant short- and medium-term regional temperature changes. The CO_2 emissions would cause long-term warming. The CO_2 emissions from such a conflict are projected to be 92 to 690 Tg-CO_2.

The annual electricity production due to nuclear energy in 2017 was 2,506 TWh/y. If that doubled to 5,000 TWh/y and if one nuclear exchange, as described above, resulted during a 100 year period, the net carbon emissions due to nuclear weapons proliferation caused by the expansion of nuclear energy worldwide would be 0.2 to 1.4 g-CO_2/kWh. This calculation assumes that the total energy generation is 5,000 TWh/y multiplied by 100 years. The resulting emission rate depends on the probability of a nuclear exchange over a given period and the strengths of nuclear devices used. The probability is bounded between 0 and 1 exchange over 100 years to give the range of possible emissions for one such event as 0 to 1.4 g-CO_2e/kWh, which is the emission rate used in Table 3.5.

3.3.2.2. Meltdown Risk

The second risk of nuclear power related to energy security is meltdown risk. As stated in Section 3.3.2.1, the Intergovernmental Panel on Climate Change points to **operational risks** (meltdown) as a barrier and risk associated with nuclear power.

Through 2019, about 1.5 percent of all nuclear reactors operating in history have had a partial or significant core meltdown. To date, meltdowns at nuclear power plants have been either catastrophic (Chernobyl, Russia in 1986; three reactors at Fukushima Dai-ichi, Japan in 2011) or damaging (Three-Mile Island, Pennsylvania in 1979; Saint-Laurent France in 1980). The nuclear industry has proposed new reactor designs that they suggest are safer. However, these designs are generally untested, and there is no guarantee that the reactors will be designed, built and operated correctly or that a natural disaster or act of terrorism, such as an airplane flown into a reactor, will not cause the reactor to fail, resulting in a major disaster.

On March 11, 2011, an earthquake measuring 9.0 on the Richter scale, and the subsequent tsunami that knocked out backup power to a cooling system, caused six nuclear reactors at the **Fukushima 1 Dai-ichi plant** in northeastern Japan to shut down. Three reactors experienced a significant meltdown of nuclear fuel rods and multiple explosions of hydrogen gas that had formed during efforts to cool the rods with seawater. Uranium fuel rods in a fourth reactor also lost their cooling. As a result, cesium-137, iodine-131, and other radioactive particles and gases were released into the air. Locally, tens of thousands of people were exposed to the radiation, and 170,000 to 200,000 people were evacuated from their homes. 1,600 to 3,700 people perished during the evacuation alone (Johnson, 2015; Denyer, 2019). At least one nuclear plant worker died from lung cancer from direct radiation exposure (BBC News, 2018).

The radiation release created a dead zone around the reactors that may not be safe to inhabit for decades to centuries. The radiation also poisoned the water and food supplies in and around Tokyo. The radiation

plume from the plant spread worldwide within a week. Radioactivity spread worldwide, although levels in Japan within 100 km of the plant were extremely high, those in the rest of Japan and eastern China were lower, and those in North America and Europe were even lower (Ten Hoeve and Jacobson, 2012). It is estimated that 130 (15 to 1,100) cancer related mortalities and 180 (24 to 1,800) cancer-related morbidities will occur worldwide, primarily in eastern Asia, over the next several decades due to the meltdown (Ten Hoeve and Jacobson, 2012). The cost of the cleanup of the Fukushima reactors and the surrounding area is estimated at $460 to $640 billion (Denyer, 2019), equivalent to about $1.2 billion for every nuclear reactor that exists worldwide.

The 1.5 percent risk of a catastrophe due to nuclear power plants is a high risk. Catastrophic risks with all WWS technologies aside from large hydropower (due to the risk of dam collapse) are zero. WWS roadmaps do not call for an increase in the number of large hydropower dams worldwide, only a more effective use of existing ones.

3.3.2.3. Radioactive Waste Risks

Another risk associated with nuclear power is the risk of human and animal exposure to radioactivity from fuel rods consumed by once-through nuclear reactors. Such fuel rods, once consumed, are considered **radioactive waste**. Currently, most fuel rods are stored at the same site as the reactor that consumed them. This has given rise to hundreds of radioactive waste sites in many countries that must be maintained for at least 200,000 years, far beyond the lifetimes of any nuclear power plant. Plans in the United States, which houses about one quarter of all nuclear reactors worldwide, to store the waste inside of Yucca Mountain, have not been approved. The more nuclear waste accumulates, the greater the risk of radioactive leaks, which can damage water supply, crops, animals, and humans.

3.3.2.4. Uranium Mining Health Risks and Land Degradation

The final risks discussed related to nuclear power are the risk of lung cancer by miners and land degradation due to uranium mining. Such risks continue so long as nuclear power plants continue to operate because the plants need uranium to produce electricity. WWS technologies, on the other hand, do not require the continuous mining of any material, only one-time mining to produce the WWS devices. As such, WWS technologies do not have this risk.

Uranium mining causes lung cancer in large numbers of miners because uranium mines contain natural radon gas, some of whose decay products are carcinogenic. Several studies have found a link between high radon levels and cancer (e.g., Henshaw et al., 1990; Lagarde et al., 1997). A study of 4,000 uranium miners between 1950 and 2000 (CDC, 2000) found that 405 (10 percent) died of lung cancer, a rate six times that expected based on smoking rates alone. 61 others died of mining related lung diseases, supporting the hypothesis that uranium mining is unhealthy. In fact, the combination of radon and cigarette smoking increases lung cancer risks above the normal risks associated with smoking (Hampson et al., 1998). Clean, renewable energy does not have this risk because (a) it does not require the continuous mining of any material, only one-time mining to produce the energy generators; and (b) the mining does not carry the same lung cancer risk that uranium mining does.

Radon (**Rn**) is a radioactive but chemically unreactive, colorless, tasteless, and odorless gas that forms naturally in soils. The source of radon gas is the radioactive decay of ^{238}U. Radon formation from uranium involves a long sequence of radioactive decay processes. During radioactive decay of an element, the element spontaneously emits radiation in the form of an alpha (α) particle, beta (β) particle, or gamma (γ) ray. An **alpha particle** is the nucleus of a helium atom, which is made of two neutrons and two protons. It is the least penetrating form of radiation and can be stopped by a thick piece of paper. Alpha particles are not dangerous unless the emitting substance is inhaled or ingested. A **beta particle** is a high-velocity electron. Beta particles penetrate deeper than do alpha particles, but less than do other forms of radiation, such as gamma rays. A **gamma ray** is a highly energized, deeply penetrating photon emitted from the nucleus of an atom not only during nuclear fusion (e.g., in the sun's core), but also sometimes during radioactive decay of an element.

The French physicist **Antoine Henri Becquerel** (1871 to 1937) discovered radioactive decay on March 1, 1896. Becquerel placed a uranium-containing mineral on top of a photographic plate wrapped by thin, black paper. After letting the experiment sit in a drawer for a few days, he developed the plate and found that it had become fogged by emissions, which he traced to the uranium in the mineral. He referred to the emissions as **metallic phosphorescence**. What he had discovered was the emission of some type of particle due to radioactive decay. He repeated the experiment by placing coins under the paper and found that their outlines were traced by the emissions. Two years later, the New Zealand-born, British physicist **Ernest Rutherford** (1871 to 1937) found that uranium emitted two types of particles, which he named alpha and beta particles. Rutherford later discovered the gamma ray as well.

Equation 3.11 summarizes the radioactive decay pathway of ^{238}U to ^{206}Pb. Numbers shown are half-lives of each decay process.

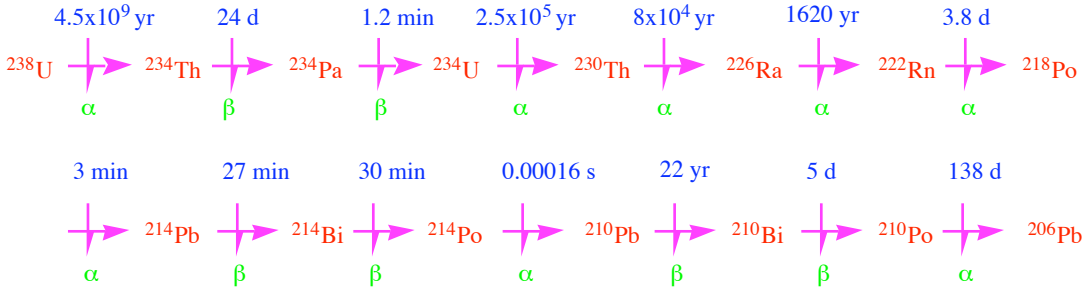

(3.11)

When it decays to produce radon, ^{238}U first releases an alpha particle, producing thorium-234 (^{234}Th), which decays to protactinium-234 (^{234}Pa), releasing a beta particle. ^{234}Pa has the same number of protons and neutrons in its nucleus as does ^{234}Th, but ^{234}Pa has one less electron than does ^{234}Th, giving ^{234}Pa a positive charge. ^{234}Pa decays further to uranium-234 (^{234}U), then to thorium-230 (^{230}Th), then to radium-226 (^{226}Ra), and then to radon-222 (^{222}Rn).

Whereas radon precursors are bound in minerals, ^{222}Rn is a gas that can be breathed in. ^{222}Rn has a half-life of 3.8 days. It decays to polonium-218 (^{218}Po), which has a half-life of 3 minutes and decays to lead-214 (^{214}Pb). ^{218}Po and ^{214}Pb, referred to as **radon progeny**, are electrically charged and can be inhaled or attach to particles that are inhaled. In the lungs or in ambient air, ^{214}Pb decays to bismuth-214 (^{214}Bi), which decays to polonium-214 (^{214}Po). ^{214}Po decays almost immediately to lead-210 (^{210}Pb), which has a lifetime of 22 years and usually settles to the ground if it has not been inhaled. It decays to bismuth-210 (^{210}Bi), then to polonium-210 (^{210}Po), and then to the stable isotope, lead-206 (^{206}Pb), which does not decay further.

^{222}Rn, a gas, is not itself harmful, but its progeny, ^{218}Po and ^{214}Pb, which enter the lungs directly or on the surfaces of aerosol particles, are highly carcinogenic (Polpong and Bovornkitti, 1998). Any activity, such as uranium mining, increasing the inhalation of aerosol particles (e.g., dust) enhances the risk of inhaling radon progeny. As such, exposure of uranium miners to radon is another risk associated with nuclear energy.

Like with coal, oil, and natural gas mining, uranium mining also despoils land and reduces the carbon stored in soil. In 2017, 19 countries mined uranium. Kazakhstan, Canada, Australia, Namibia, and Niger produced the most uranium. Mines can be open pit or underground. Open pit mines cause the most land degradation. Table 3.5 provides an estimate of the effective CO_2e emissions due to clearing vegetation from land for uranium mining associated with nuclear power. The continuous mining for fuels is not needed in a 100 percent WWS world.

3.2.2. Total CO_2e Emissions of Energy Technologies

Lifecycle emissions are one component of total carbon equivalent (CO_2e) emissions. Additional components relevant to fossil fuels with carbon capture include opportunity cost emissions, anthropogenc heat emissions, anthropogenic water vapor emissions, emissions risk due to CO_2 leakage, and emissions due to covering or clearing land for energy development. These are discussed next, in turn.

3.2.2.1. Opportunity Cost Emissions

Opportunity cost emissions are emissions from the background electric power grid, averaged over a defined period of time (e.g., either 20 years or 100 years), due to two factors. The first factor is the longer time lag between planning and operation of one energy technology relative to another. The second factor is the longer downtime needed to refurbish one technology at the end of its useful life when its useful life is shorter than that of another technology (Jacobson, 2009).

For example, if Plant A takes 4 years and Plant B takes 10 years between planning and operation, the background grid will emit pollution for 6 more years out of 100 years with Plant B than with Plant A. The emissions during those additional 6 years are opportunity cost emissions. Such additional emissions include emissions of both health- and climate-affecting air pollutants.

Similarly, if Plant A and B have the same planning-to-operation time but Plant A has a useful life of 20 years and requires 2 years of refurbishing to last another 20 year and Plant B has a useful life of 30 years but takes only 1 year of refurbishing, then Plant A is down 2 y / 22 y = 9.1 percent of the time for refurbishing and Plant B is down 1 y / 31 y = 3.2 percent of the time for refurbishing. As such, Plant B is down an additional (0.091 – 0.032) × 100 y = 5.9 years out of every 100 for refurbishing. During those additional years, the background grid will emit pollution with Plant B.

Mathematically, opportunity cost emissions (E_{OC}, in g-CO_2e/kWh) are calculated as

$$E_{OC} = E_{BR,H} - E_{BR,L} \quad (3.1)$$

where $E_{BR,H}$ are total background grid emissions over a specified number of years due to delays between planning and operation and downtime for refurbishing of the technology with the more delays. $E_{BR,L}$ is the same but for the technology with the fewer delays. Background emissions (for either technology) over the number of years of interest, Y, are calculated as

$$E_{BR} = E_G \times ([T_{PO} + (Y - T_{PO}) \times T_R / (L+T_R)] / Y \quad (3.2)$$

where E_G is the emissions intensity of the background grid (g-CO_2e/kWh for analyses of the climate impacts and g-pollutant/kWh for analyses of health-affecting air pollutants), T_{PO} is the time lag (in years) between planning and operation of the technology, T_R is the times (years) to refurbish the technology, and L is the operating life (years) of the technology before it needs to be refurbished.

Example 3.1. Opportunity cost emissions.
What are the opportunity cost emissions (g-CO_2e/kWh) over 100 years resulting from Plant B if its planning-to-operation time is 15 years, its lifetime is 40 years, and its refurbishing time is 3 years, whereas these values for Plant A are 3 years, 30 years, and 1 year, respectively? Assume both plants produce the same number of kWh/y once operating, and the background grid emits 550 g-CO_2e/kWh.

Solution:
The opportunity cost emissions are calculated as the emissions from the background grid over 100 years of the plant with the higher background emissions (Plant B in this case) minus those from the plant with the lower background emissions (Plant A).

The background emissions from Plant B are calculated from Equation 3.2 with E_G=550 g-CO_2e/kWh, Y=100 y, T_{PO}=15 y, L=40 y, and T_R=3 y as $E_{BR,H}$=550 g-CO_2e/kWh × [15 y + (100 y – 15 y) × 3 y / 43 y)] / 100 y = 115 g-CO_2e/kWh.

Similarly, the background emissions from Plant A averaged over 100 years are $E_{BR,L}$=550 g-CO_2e/kWh × [3 y + (100 y – 3 y) × 1 y / 31 y)] / 100 y = 33.7 g-CO_2e/kWh. The difference between the two from Equation 3.1, E_{OC}= $E_{BR,H}$-$E_{BR,L}$= 81.3 g-CO_2e/kWh, is the opportunity cost emissions of Plant B over 100 years.

The time lag between planning and operation of a technology includes a development time and construction time. The development time is the time required to identify a site, obtain a site permit, purchase or lease the land, obtain a construction permit, obtain financing and insurance for construction, install transmission, negotiate a power purchase agreement, and obtain permits. The construction period is the period of building the plant, connecting it to transmission, and obtaining a final operating license.

The development phase of a coal-fired power plant without carbon capture equipment is generally 1 to 3 years, and the construction phase is another 5 to 8 years, for a total of 6 to 11 years between planning and operation (Jacobson, 2009). No coal plant has been built from scratch with carbon capture, so this could add to the planning-to-operation time. However, for a new plant, it is assumed that the carbon capture equipment can be added during the long planning-to-operation time of the coal plant itself. As such, Table 3.5 assumes the planning-to-operation time of a coal plant without carbon capture is the same as that with carbon capture. The typical lifetime of a coal plant before it needs to be refurbished is 30 to 35 years. The refurbishing time is an estimated 2 to 3 years.

No natural gas plant with carbon capture exists. The estimated planning-to-operation time of a natural gas plant without carbon capture is less than that of a coal plant. However, because of the shorter time, the addition of carbon capture equipment to a new natural gas plant is likely to extend its planning-to-operation time to that of a coal plant with or without carbon capture (6 to 11 years).

For comparison, the planning-to-operation time of a utility-scale wind or solar farm is generally 3 to 5 years, with a development period of 1 to 3 years and a construction period of 1 to 2 years (Jacobson, 2009).

This time applies to both onshore and offshore wind. For example, the 407 MW (49 turbine) Horns Rev 3 offshore wind farm, located in the North Sea off of the west coast of Denmark, required 1 year and 10 months to build (Frangoul, 2019). Wind turbines often last 30 years before refurbishing, and the refurbishing time is 0.25 to 1 year.

Table 3.5 provides the estimate opportunity cost emissions of coal and natural gas with carbon capture due to the time lag between planning and operation of those plants relative to wind or solar farms. The table indicates an investment in fossil fuels with carbon capture instead of wind and solar result in an additional 46 to 62 g-CO_2e/kWh in opportunity cost emissions from the background grid.

Table 3.5. Total 100-year CO_2e emissions from several different energy technologies. The total includes lifecycle emissions, opportunity cost emissions, anthropogenic heat and water vapor emissions, weapons and leakage risk emissions, and emissions from loss of carbon storage in land and vegetation. All units are g-CO_2e/kWh-electricity, except the last, column, which gives the ratio of total emissions of a technology to the emissions from onshore wind. CCS/U is carbon capture and storage or use.

Technology	[a]Lifecycle emissions	[b]Opportunity cost emissions due to delays	[c]Anthro-pogenic heat emissions	[d]Anthro-pogenic water vapor emissions	[e]Nuclear Weapons risk or 100-Year CCS/U leakage risk	[f]Loss of CO_2 due to covering land or clearing vegetation	**[g]Total 100-year CO_2e**	**Ratio of 100-year CO_2e to that of wind-onshore**
Solar PV-rooftop	15-34	-12 to -16	-2.2	0	0	0	**0.8-15.8**	**0.1-3.3**
Solar PV-utility	10-29	0	-2.2	0	0	0.054-0.11	**7.85-26.9**	**0.91-5.6**
CSP	8.5-24.3	0	-2.2	0 to 2.8	0	0.13-0.34	**6.43-25.2**	**0.75-5.3**
Wind-onshore	7.0-10.8	0	-1.7 to -0.7	-0.5 to -1.5	0	0.0002-0.0004	**4.8-8.6**	**1**
Wind-offshore	9-17	0	-1.7 to -0.7	-0.5 to -1.5	0	0	**6.8-14.8**	**0.79-3.1**
Geothermal	15.1-55	14-21	0	0 to 2.8	0	0.088-0.093	**29-79**	**3.4-16**
Hydroelectric	17-22	41-61	0	2.7 to 26	0	0	**61-109**	**7.1-22.7**
Wave	21.7	4-16	0	0	0	0	**26-38**	**3.0-7.9**
Tidal	10-20	4-16	0	0	0	0	**14-36**	**1.6-7.5**
Nuclear	9-70	64-102	1.6	2.8	0-1.4	0.17-0.28	**78-178**	**9.0-37**
Biomass	43-1,730	36-51	3.4	3.2	0	0.09-0.5	**86-1,788**	**10-373**
Natural gas-CCS/U	179-405	46-62	0.61	3.7	0.36-8.6	0.41-0.69	**230-481**	**27-100**
Coal-CCS/U	230-935	46-62	1.5	3.6	0.36-8.6	0.41-0.69	**282-1,011**	**33-211**

[a]Lifecycle emissions are 100-year carbon equivalent (CO_2e) emissions that result from the construction, operation, and decommissioning of a plant. They are determined as follows:

Solar PV-rooftop: The range is assumed to be the same as the solar PV-utility range, but with 5 g-CO_2/kWh added to both the low and high ends to account for the use of fixed tilt for all rooftop PV versus the use of some tracking for utility PV.

Solar PV-utility: The range is derived from Fthenakis and Raugei (2017). It is inclusive of the 17 g-CO_2/kWh mean for CdTe panels at 11 percent efficiency, the 27 g-CO_2e/kWh mean for multi-crystalline silicon panels at 13.2 percent efficiency, and the 29 gCO_2e/kWh mean for mono-crystalline silicon panels at 14 percent efficiency. The upper limit of the range is held at the mean for multi-crystalline silicon since panel efficiencies are now much higher than 13.2 percent. The lower limit is calculated by scaling the CdTe mean to 18.5 percent efficiency, its maximum in 2018.

CSP: The lower limit CSP lifecycle emission rate is from Jacobson (2009). The upper limit is from Ko et al. (2018).

Wind-onshore and wind-offshore: The range is derived from Kaldelis and Apostolou (2017).

Geothermal: The range is from Jacobson (2009) and consistent with the review of Tomasini-Montenegro et al. (2017).

Hydroelectric and wave: From Jacobson (2009).

Tidal: From Douglass et al. (2008).

Nuclear: The range of 9-70 g-CO_2e/kWh is from Jacobson (2009), which is within the Intergovernmental Panel on Climate Change (IPCC)'s range of 4-110 g-CO_2e/kWh (Bruckner et al., 2014), and conservative relative to the 68 (10-130) g-CO_2e/kWh from the review of Lenzen (2008) and the 66 (1.4-288) g-CO_2e/kWh from the review of Sovacool (2008).

Biomass: The range provided is for biomass electricity generated by forestry residues (43 gCO_2e/kWh), industry residues (46), energy crops (208), agriculture residues (291), and municipal solid waste (1730) (Kadiyala et al., 2016).

Natural gas-CCS/U: The lower bound is for the CCGT with carbon capture plant from Skone (2015), also provided in Table 3.4. The upper bound is CCGT value without carbon capture, 506 g-CO_2e/kWh from Table 3.4, multiplied by 80 percent, which is the percent of CO_2e emissions expected to be captured from the Petra Nova facility that will remain in the air over 100 years (Table 3.6).

Coal-CCS/U: The lower bound is for IGCC with carbon capture from Skone (2015). The upper bound is the coal value without carbon capture, 1,168 g-CO_2e/kWh from Table 3.6, multiplied by 80 percent, which is the percent of coal lifecycle CO_2e emissions from the Petra Nova facility that will remain in the air over 100 years (Table 3.6).

[b]Opportunity cost emissions are emissions per kWh over 100 years from the background electric power grid, calculated from Equations 3.1 and 3.2 due to (a) the longer time lag between planning and operation of one energy technology relative to another and (b) additional downtime to refurbish a technology at the end of its useful life compared with the other technology. The planning-to-operation times of the technologies in this table are 0.5-2 years for solar PV-rooftop; 2-5 years for solar PV-utility, CSP, wind-onshore, wind-offshore, tidal, and wave; 3-6 years for geothermal; 8-16 years for hydroelectric; 10-19 years for nuclear; 4-9 years for biomass (without CCS/U), and 6-11 years for natural gas-CCS/U and coal-CCS/U (Jacobson, 2009, except rooftop PV and natural gas-CCS/U values are added and solar PV-rooftop is updated here). The refurbishment times are 0.05-1 year for solar PV-rooftop; 0.25-1 year for solar-PV-utility, CSP, wind-onshore, wind-offshore, wave, and tidal; 1-2 years for geothermal and hydroelectric; 2-4 years for nuclear, and 2-3 years for biomass, coal-CCS/U, and natural gas-CCS/U. The lifetimes before refurbishment are 15 years for tidal and wave; 30 years for solar PV-rooftop, solar PV-utility, CSP, wind-onshore, wind-offshore; 30-35 years for biomass, coal-CCS/U, and natural gas-CCS/U; 30-40 years for geothermal; 40 years for nuclear; and 80 years for hydroelectric (Jacobson, 2009). The opportunity cost emissions are calculated here relative to the utility-scale technologies with the shortest time between planning and operation (solar-PV-utility, CSP, wind-onshore, and wind-offshore). The opportunity cost emissions of the latter technologies are, by definition, zero. The opportunity cost emissions of all other technologies are calculated like in Example 3.1 while assuming a background U.S. grid emission intensity equal to 557.3 g-CO_2e/kWh in 2017. This is derived from an electricity mix from EIA (2018d) and emissions, weighted by their 100-year GWPs, of CO_2, CH_4, and N_2O from mining, transporting, processing and using fossil fuels, biomass, or uranium. The reason tidal power has opportunity cost emissions although its planning-to-operation time is the same as onshore wind is the shorter lifetime of tidal turbines than wind turbines. Thus, tidal has more down time over 100 years than do other technologies. See Section 3.2.2.1. The opportunity cost emissions of offshore and onshore wind are assumed to be the same because new projects suggest offshore wind, particularly with faster assembly techniques and with floating turbines, are easier to permit and install now than a decade ago. Although natural gas plants don't take so long as coal plants between planning and operation, natural gas combined with CCS/U is assumed to take the same time as coal with CCS/U.

[c]Anthropogenic heat emissions here include the heat released to the air from combustion (for coal or natural gas) or nuclear reaction, converted to CO_2e (see Section 3.2.2.2). For solar PV and CSP, heat emissions are negative because these three technologies reduce sunlight to the surface by converting it to electricity. The lower flux to the surface cools the ground or a building below the PV panels. For wind turbines, heat emissions are negative because turbines extract energy from wind to convert it to electricity (Section 3.2.2.3 and Example 3.6). For binary geothermal plants (low end), it is assumed all heat is re-injected back into the well. For non-binary plants, it is assumed that some heat is used to evaporate water vapor (thus the anthropogenic water vapor flux is positive) but remaining heat is injected back into the well. The electricity from all electric power generation also dissipates to heat, but this is due to the consumption rather than production of power and is the same amount per kWh for all technologies so is not included in this table.

[d]Anthropogenic water vapor emissions here include the water vapor released to the air from combustion (for coal and natural gas) or from evaporation (water-cooled CSP, water-cooled geothermal, hydroelectric, nuclear natural gas, and coal), converted to CO_2e (see Section 3.2.2.3). Air-cooled CSP and geothermal plants have zero water vapor flux, representing the low end of these technologies. The high end is assumed to be the same as for nuclear, which also uses water for cooling. The low end for hydroelectric power assumes 1.75 kg-H_2O/kWh evaporated from reservoirs at mid to high latitudes (Flury and Frischknecht, 2012). The upper end is 17.0 kg-H_2O/kWh from Jacobson (2009) for lower latitude reservoirs and assumes reservoirs serve multiple purposes. For biomass, the number is based only on the water emitted from the plant due to evaporation or combustion, not water to irrigate some energy crops. Thus, the upper estimate is low. The negative water vapor flux for onshore and offshore wind is due to the reduced water evaporation caused by wind turbines (Section 3.2.2.3 and Example 3.6).

[e]Nuclear weapons risk is the risk of emissions due to nuclear weapons use resulting from weapons proliferation caused by the spread of nuclear energy. The risk ranges from zero (no use of weapons over 100 years) to 1.4 g-CO_2e/kWh (one nuclear exchange in 100 years) (Section 3.3.2.1). The 100-year CCS/U leakage risk is the estimated rate,

averaged over 100 years, that CO_2 sequestered underground leaks back to the atmosphere. Section 3.2.2.4 contains a derivation. The leakage rate from natural gas-CCS/U is assumed to be the same as for coal-CCS/U.

[f]Loss of carbon, averaged over 100 years, due to covering land or clearing vegetation is the loss of carbon sequestered in soil or in vegetation due to the covering or clearing land by an energy facility; by a mine where the fuel is extracted from (in the case of fossil fuels and uranium); by roads, railways, or pipelines needed to transport the fuel; and by waste disposal sites. No loss of carbon occurs for solar PV-rooftop, wind-offshore, wave, or tidal power. In all remaining cases, except for solar PV-utility and CSP, the energy facility is assumed to replace grassland with the organic carbon content and grass content as described in the text. For solar PV-utility and CSP, it is assumed that the organic content of both the vegetation and soil are 7 percent that of grassland because (a) most all CSP and many PV arrays are located in deserts with low carbon storage and (a) most utility PV panels and CSP mirrors are elevated above the ground. For biomass, the low value assumes the source of biomass is industry residues or contaminated wastes. The high value assumes energy crops, agricultural residues, or forestry residues. See Section 3.2.2.5.

[g]The total column is the sum of the previous six columns.

3.2.2.2. Anthropogenic Heat Emissions

Anthropogenic heat emissions were defined in Section 1.2.3 to include the heat released to the air from the dissipation of electricity; from the dissipation of motive energy by friction; from the combustion of fossil fuels, biofuels and biomass for energy; from nuclear reaction; and from anthropogenic biomass burning. Jacobson (2014) provide the relative contributions of different energy generating technologies to worldwide anthropogenic heat emissions.

Table 3.5 includes the g-CO_2e/kWh emissions from heat of combustion (for biomass, natural gas, and coal) and from nuclear reaction. However, because the dissipation of the resulting electricity back to heat is due to the consumption rather than production of electricity, that heat release term is not included in the table. In any case, the heat released per unit electricity produced is the same for all technologies.

Solar PV and CSP convert solar radiation to electricity, thereby reducing the flux of heat to the ground or to rooftops below PV panels. This is reflected in Table 3.5 as a negative heat flux. Wind turbines also cause a negative heat flux, discussed in Section 3.2.2.3.

The CO_2e emissions (g-CO_2e/kWh) due to the anthropogenic heat flux is calculated for all technologies (including the negative heat fluxes due to solar and wind) as follows:

$$H = E_{CO2} \times A_h / (F_{CO2} \times G_{elec}) \quad (3.3)$$

where E_{CO2} is the equilibrium global anthropogenic emission rate of CO_2 (g-CO_2/y) that gives a specified anthropogenic mixing ratio of CO_2 in the atmosphere, F_{CO2} is the direct radiative forcing (W/m^2) of CO_2 at the specified mixing ratio, A_h is the anthropogenic heat flux (W/m^2) due to a specific electric power producing technology, and G_{elec} is the annual global energy output of the technology (kWh/y).

The idea behind this equation is that the current radiative forcing (W/m^2) in the atmosphere due to CO_2 can be maintained at an equilibrium CO_2 emission rate,

$$E_{CO2} = \chi_{CO2} C / \tau_{CO2} \quad (3.4)$$

where χ_{CO2} (ppmv) is the specified anthropogenic mixing ratio that gives the current CO_2 radiative forcing, C is a conversion factor (8.0055×10^{15} g-CO_2/ppmv-CO_2), and τ_{CO2} is the data-constrained *e*-folding lifetime of CO_2 against loss by all processes. As of 2019, τ_{CO2} is ~50 years but increasing over time (e.g., Jacobson, 2012a).

Equation 3.4 is derived by noting that the time rate of change of the atmospheric mixing ratio of a well-mixed gas, such as CO_2 is simply, $d\chi/dt = E - \chi C/\tau$. In steady state, this simplifies to $E=\chi C/\tau$. Scaling the

ratio of this equilibrium CO_2 emission rate to the radiative forcing of CO_2 by the ratio of the anthropogenic heat flux to the electricity generation per year producing that heat flux, gives Equation 3.3, the CO_2e emission rate of the heat flux.

Thus, Equation 3.3 accounts for the emission rate of CO_2 needed to maintain a mixing ratio of CO_2 in the air that gives a specific radiative forcing. It does not use the present day emission rate because that results in a much higher CO_2 mixing ratio than is currently in the atmosphere because CO_2 emissions are not in equilibrium with the CO_2 atmospheric mixing ratio. Equation 3.3 requires a constant emission rate that gives the observed mixing ratio of CO_2 for which the current direct radiative forcing applies. Similarly, the energy production rate in Equation 3.3 gives a consistent anthropogenic heat flux.

Finally, whereas radiative forcing is a top-of-the-atmosphere value (and represents changes in heat integrated over the whole atmosphere) and heat flux is added to the bottom of the atmosphere, they both represent the same amount of heat added to the atmosphere. In fact, because the anthropogenic heat flux adds heat to near-surface air, it has a slightly greater impact on surface air temperature per unit radiative forcing than does CO_2. For example, the globally averaged temperature change per unit direct radiative forcing for CO_2 is ~0.6 K/(W/m^2) (Jacobson, 2002), whereas the temperature change per unit anthropogenic heat plus water vapor flux is ~0.83 K/(W/m^2) (Jacobson, 2014). As such, the estimated CO_2e values for heat fluxes in particular in Table 3.5 may be slightly underestimated.

Example 3.2. Calculate the carbon equivalent heat emissions for coal and nuclear power worldwide.
In 2005, the anthropogenic flux of heat (aside from heat used to evaporate water) from all anthropogenic heat sources worldwide was A_h=0.027 W/m^2 (Jacobson, 2014). Assume the percent of all heat from coal combustion was 4.87 percent and from nuclear reaction was 1.55 percent.

Estimate the CO_2e emissions corresponding to the coal and nuclear heat fluxes given the energy generation of $G_{elec}=8.622\times10^{12}$ kWh/y from coal combustion and 2.64×10^{12} kWh/y from nuclear reaction.

Assume an anthropogenic CO_2 direct radiative forcing of F_{CO2}=1.82 W/m^2, which corresponds to an anthropogenic mixing ratio of CO_2 of χ_{CO2}=113 ppmv (Myhre et al., 2013). Also assume a CO_2 *e*-folding lifetime of τ_{CO2}=50 years.

Solution:
From Equation 3.4, the equilibrium emission rate of CO_2 giving the anthropogenic mixing ratio is

$E_{CO2}=1.809\times10^{16}$ g-CO_2/y.

Multiplying the total anthropogenic heat flux by the respective fractions of heat from coal combustion and nuclear reaction gives A_h=0.00132 W/m^2 for coal and 0.00042 W/m^2 for nuclear. Substituting these and the other given values into Equation 3.3 gives H = 1.52 g-CO_2e/kWh for coal and 1.57 g-CO_2/kWh for nuclear.

Example 3.3. Calculate the carbon-equivalent negative heat emissions of a solar PV panel.
Solar panels convert about 20 percent of the sun's energy to electricity, thereby reducing the flux of sunlight to the ground. What is the reduction in heat flux (W/m^2) per kWh/y of electricity generated by a solar panel and what is the corresponding CO_2e emission reduction? The surface area of the Earth is 5.092×10^{14} m^2.

Solution:
If a solar panel produces G_{elec}=1 kWh/y of electricity, the panel prevents exactly that much solar radiation from converting to heat compared with the sunlight otherwise hitting an equally reflective surface. Eventually, the electricity converts to heat as well (as does the electricity from all electric power generators). However, other electric power generators do not remove heat from the sun on the same timescale as solar panels do.

Multiplying the avoided heat (-1 kWh/y) by 1,000 W/kW and dividing by 8760 h/y and by the area of the Earth gives $A_h=-2.24\times10^{-16}$ W/m^2. Substituting this, G_{elec}=1 kWh/y, and E_{CO2} and F_{CO2} from Example 3.2 into Equation 3.3 gives H=-2.23 g-CO_2e/kWh.

Finally, for hydropower, evaporation of water vapor at the surface of a reservoir by the sun increases anthropogenic water vapor emissions (Section 3.2.2.3). Because evaporation requires energy, it cools the surface of the reservoir. The energy used to evaporate the water becomes embodied in latent heat carried by the water vapor. However, the water vapor eventually condenses in the air (forming clouds), releasing the heat back to the air. As a result, warming of the air offsets cooling at the surface, so hydropower causes no net anthropogenic heat flux. On the other hand, water vapor is a greenhouse gas, resulting in a net warming of the air due to evaporation. This warming is accounted for in the next section.

3.2.2.3. Anthropogenic Water Vapor Emissions

Fossil fuel, biofuel, and biomass burning release not only heat, but also water vapor. The water vapor results from chemical reaction between the hydrogen in the fuel and oxygen in the air. In addition, coal, natural gas, and nuclear plants require cool liquid water to re-condense the hot steam as it leaves a steam turbine. This process results in significant water evaporating out of a cooling tower to the sky. Many CSP turbines also use water cooling although some use air cooling. Similarly, whereas non-binary geothermal plants and some binary plants use water cooling, thus emit water vapor, binary plants that use air cooling do not emit any water vapor. Further, water evaporates from reservoirs behind hydroelectric power plant dams. Table 1.1 indicates that anthropogenic water vapor from all anthropogenic sources causes about 0.23 percent of global warming.

On the other hand, wind turbines reduce water vapor, a greenhouse gas, by reducing wind speeds (Chapter 7) (Jacobson and Archer, 2012; Jacobson et al., 2018a). Water evaporation is a function of wind speed (and temperature).

In this section, the positive or negative CO_2e emissions per unit energy (M, g-CO_2e/kWh) due to increases or decreases in water vapor fluxes resulting from an electric power source are quantified. The emissions are estimated with an equation similar to Equation, 3.3, except with the anthropogenic moisture energy flux (A_m, W/m^2) is substituted for the heat flux:

$$M = E_{CO2} \times A_m / (F_{CO2} \times G_{elec}) \quad (3.5)$$

In this equation, the globally averaged moisture energy flux can be obtained from the water vapor flux per unit energy (V, kg-H_2O/kWh) by

$$A_m = V \times L_e \times G_{elec} / (S \times A_e) \quad (3.6)$$

where L_e=2.465×10^6 J/kg-H_2O is the latent heat of evaporation, S=3.1536×10^7 seconds per year, and A_e=5.092×10^{14} m^2 is the surface area of the Earth. For water evaporating from a hydropower reservoir, V = 1.75 to 17 kg-H_2O/kWh (Table 3.5, footnote c).

Combining Equations 3.5 and 3.6 gives the globally averaged CO_2e emissions per unit energy due to a positive or negative water vapor flux resulting from an energy generator as

$$M = E_{CO2} \times V \times L_e / (F_{CO2} \times S \times A_e) \quad (3.7)$$

This equation is independent of the total annual energy production (G_{elec}). Examples 3.4 to 3.6 provide calculations of anthropogenic water vapor fluxes for several of the generators in Table 3.5.

Example 3.4. Calculate the carbon-equivalent anthropogenic water vapor emissions from natural gas and nuclear plants.

The global anthropogenic water vapor flux from natural gas power plants in 2005 was A_m=0.00268 W/m^2 and from nuclear power plants was A_m=0.000746 W/m^2 (Jacobson, 2014). The total energy generation from natural gas use was G_{elec}=7.208×10^{12} kWh/y and from nuclear was 2.64×10^{12} kWh/y. Calculate the CO_2e emissions associated with these fluxes.

Solution:
Substituting E_{CO2} and F_{CO2} from Example 3.2 and A_m and G_{elec} provided in the problem into Equation 3.5 gives M=3.69 g-CO_2e/kWh for natural gas and 2.81 g-CO_2e/kWh for nuclear.

Example 3.5. Calculate the carbon-equivalent anthropogenic water vapor emissions from a hydropower reservoir.
If the evaporation rate of water from a hydropower reservoir is V=1.75 kg-H_2O/kWh (Flury and Frischknecht, 2012), determine the CO_2e emissions of water vapor from the reservoir.

Solution:
Substituting V into Equation 3.7 with E_{CO2} and F_{CO2} from Example 3.2 gives the carbon equivalent emissions due to hydropower reservoir evaporation as M=2.66 g-CO_2e/kWh.

Wind turbines extract kinetic energy from the wind and convert it to electricity. **Kinetic energy** is the energy embodied in air due to its motion. For every 1 kWh of electricity produced, 1 kWh of kinetic energy is extracted. Like with all electric power generation, the 1 kWh of electricity eventually converts back to heat that is added back to the air. However, for purposes of assigning CO_2e emissions or savings, the conversion of electricity back to heat is not assigned to any particular electric power generator in Table 3.5. However, the addition or extraction of heat and water vapor by the energy technology is.

When electricity dissipates to heat, some of that heat returns to kinetic energy. Heat is **internal energy**, which is the energy associated with the random, disordered motion of molecules. Higher temperature molecules move faster than lower temperature molecules. Some of the internal energy in the air causes air to rise since warm, low-density air rises when it is surrounded by cool, high-density air. To raise the air, internal energy is converted to **gravitational potential energy (GPE)**, which is the energy required to lift an object of a given mass against gravity a certain distance. The lifted parcel is now cooler as a result of giving away some of its internal energy to GPE. Differences in GPE over horizontal distance create a pressure gradient, which recreates some kinetic energy in the form of wind (Section 6.8).

In sum, wind turbines convert kinetic energy to electricity, which dissipates to heat. Some of that heat converts to GPE, some of which converts back to kinetic energy. If a wind turbine did not extract kinetic energy from the wind, that energy would otherwise still dissipate to heat due to the wind bashing into rough surfaces, which are sources of friction. But such dissipation would occur over a longer time.

However, **wind turbines have an additional effect, which is to reduce water vapor, a greenhouse gas**. When wind from dry land blows over a lake, for example, the dry wind sweeps water vapor molecules away from the surface of the lake. More water vapor molecules must then evaporate from the lake to maintain saturation of water over the lake surface. In this way, winds increase the evaporation of water over not only lakes, but also over oceans, rivers, streams, and soils. Because a wind turbine extracts energy from the wind, it slows the wind, reducing evaporation of water.

By reducing evaporation, wind turbines warm the water or soil near the turbine because evaporation is a cooling process, so less evaporation causes warming. However, because the air now contains less water vapor, less condensation occurs in the air. Since condensation releases heat, less of it means the air cools.

In addition, because a wind turbine slows the wind in its wake, it drops the air pressure in its wake as well (Section 6.4). Lower pressure decreases temperature, as evidenced by the increased fog thickness in the wake of wind turbines at the Horns Rev offshore wind farm (Hasager et al., 2013). The increase in fog

thickness results from a slight increase in the relative humidity in a turbine's wake upon a slight drop in temperature, which is due to the drop in pressure.

Thus, the surface warming due to wind turbines reducing evaporation is cancelled by the air-cooling due to both lesser atmospheric condensation and lower temperatures in the turbines wake.

However, because water vapor is a greenhouse gas, less of it in the air means that more heat radiation from the Earth's surface escapes to space, cooling the ground, reducing internal energy. Since water vapor stays in the air for days to weeks, its absence due to a wind turbine reduces heat to the surface over that time more than the one-time dissipation of electricity, created by the wind turbine, increases heat.

In sum, wind turbines allow a net escape of energy to space by reducing water vapor. A portion of the lost energy comes from the air's internal energy, resulting in lower air temperatures. The rest comes from kinetic energy, reducing wind speeds, and from gravitational potential energy, reducing air heights. As such, a new equilibrium is reached in the atmosphere. Section 6.9.1 quantifies the impacts of different numbers of turbines worldwide on temperatures and water vapor.

Thus, wind turbines reduce temperatures in the global average by reducing both heat fluxes and water vapor fluxes. Wind turbines do increase temperatures on the ground downwind of a wind farm because they reduce evaporation, but in the global average, this warming is more than offset by atmospheric cooling due to less condensation plus the loss of more heat radiation to space due to the reduction in water vapor caused by wind turbines.

The energy taken out of the atmosphere temporarily (because it is returned later as heat from dissipation of electricity) by wind turbines is 1 kWh per 1 kWh of electricity production. The maximum reduction in water vapor, based on global computer model calculations (Chapter 7), due to wind turbines ranges from -0.3 to -1 kg-H_2O/kWh, where the variation depends on the number and location of wind turbines. Example 3.6 provides an estimate of the CO_2e savings due to wind turbines from these two factors.

Example 3.6. Estimate the globally averaged CO_2e water vapor and heat emission reductions due to wind turbines.
Assuming that wind turbines extract 1 kWh of the wind's kinetic energy for each 1 kWh of electricity produced, estimate the CO_2e savings per unit energy from reduced heat and water vapor fluxes due to wind turbines considering that, when the turbine is not operating, every 1 kWh of kinetic energy in the wind evaporates 0.3 to 1 kg-H_2O/kWh and the rest of the energy remains in the atmosphere. Assume the equilibrium emission rate and resulting radiative forcing of CO_2 from Example 3.2.

Solution:
Multiplying the latent heat of evaporation (L_e=2.465×10^6 J/kg) and 1 kWh/3.6×10^6 J by -0.3 to -1 kg-H_2O/kWh gives the reduction in energy available to evaporate water as -0.21 to -0.69 kWh per kWh of electricity-produced. Multiplying 1,000 W/kW and dividing by 8760 h/y and by the area of the Earth, 5.092×10^{14} m^2, gives A_m/G_{elec} = -4.6×10^{-17} to -1.53×10^{-16} (W/m^2)/(kWh/y). Substituting this and E_{CO2} and F_{CO2} from Example 3.2 into Equation 3.5 gives the anthropogenic water vapor energy flux from wind turbines as -0.46 to -1.53 g-CO_2e/kWh.

The heat flux is the difference between -1 kWh/kWh-electricity and -0.21 to -0.69 kWh/kWh-electricity, which is -0.79 to -0.31 kWh/kWh-electricity. Performing the same calculation as above gives the anthropogenic heat flux from wind turbines as -1.77 to -0.70 g-CO_2e/kWh. The total heat plus water vapor energy flux savings due to wind turbines is thus -2.23 g-CO_2e/kWh, the same as for solar panels (Example 3.3).

3.2.2.4. Leaks of CO_2 Sequestered Underground

The sequestration of carbon underground due to CCS or CCU (e.g., from injecting CO_2 during enhanced oil recovery) runs the risk of CO_2 leaking back to the atmosphere through existing fractured rock or overly

porous soil or through new fractures in rock or soil resulting from an earthquake. Here, a range in the potential emission rate due to CO_2 leakage from the ground is estimated.

The ability of a geological formation to sequester CO_2 for decades to centuries varies with location and tectonic activity. IPCC (2005, p. 216) references CO_2 leakage rates for an enhanced oil recovery operation of 0.00076 percent per year, or 1 percent over 1,000 years, and CH_4 leakage from historical natural gas storage systems of 0.1 to 10 percent per 1,000 years. Thus, while some well-selected sites could theoretically sequester 99 percent of CO_2 for 1,000 years, there is no certainty of this since tectonic activity or natural leakage over 1,000 years is not possible to predict. Because liquefied CO_2 injected underground will be under high pressure, it will take advantage of horizontal and vertical fractures in rocks to escape as a gas back to the air. Because CO_2 is an acid, its low pH will also cause it to weather rocks over time. If a leak from an underground formation to the atmosphere occurs, it may or may not be detected. If a leak is detected, it may or may not be sealed, particularly if it occurs over a large area.

The time-averaged leakage rate of CO_2 from a reservoir can be calculated by first estimating how the stored mass of CO_2 changes over time. The stored mass (S) of CO_2 at any time t in a reservoir, resulting from a constant injection at rate I (mass/y) and e-folding lifetime against leakage, T (years), is

$$S(t)= S(0)e^{-t/T}+TI(1-e^{-t/T}) \quad (3.8)$$

where S(0) is the stored mass at time t=0. The average leakage rate over t years is then simply the injection rate minus the remaining mass stored mass at time t divided by t years,

$$L(t)= I- S(t)/t \quad (3.9)$$

Once an injection rate and lifetime against leakage are known, the average leakage rate of CO_2 from an underground storage reservoir over a specified period can be calculated from Equations 3.8 and 3.9.

Example 3.7. Estimating average leakage rates from underground storage reservoirs.
Assume a coal-fired power plant has a CO_2 emission rate before carbon capture and storage ranging from 790 to 1,017 g-CO_2/kWh. Assume also that carbon capture equipment added to the plant captures 90 and 80 percent, respectively, of the CO_2 (giving a low and high, respectively, emission rate of remaining CO_2 to the air). If the captured CO_2 is injected underground into a geological formation that has no initial CO_2 in it, calculate a low and high CO_2 emission rate from leakage averaged over 100 years, 500 years, and 1,000 years. Assume a low and high e-folding lifetime against leakage of 5,000 years and 100,000 years, respectively. The low value corresponds to 18 percent leakage over 1,000 years, close to that of some observed methane leakage rates. The high value corresponds to a 1 percent loss of CO_2 over 1,000 years (e.g., IPCC, 2005).

Solution:
The low and high injection rates are 790 × 0.9 = 711 g-CO_2/kWh and 1,017 × 0.85 = 864.5 g-CO_2/kWh, respectively. Substituting these injection rates into Equation 3.8 (using the high lifetime with the low injection rate and the low lifetime with the high injection rate) and the result into Equation 3.9 gives a leakage rate range of 0.36 to 8.6 g-CO_2/kWh over 100 years; 1.8 to 42 g-CO_2/kWh over 500 years, and 3.5 to 81 g-CO_2/kWh over 1,000 years.

Thus, the longer the averaging period, the greater the average emission rate over the period due to CO_2 leakage.

3.2.2.5. Emissions From Covering Land or Clearing Vegetation

Emissions from covering land or clearing vegetation are emissions of CO_2 itself due to (a) reducing the carbon stored in soil and in the vegetation above the soil by covering land with impervious material or (b) reducing the carbon stored in vegetation by clearing land so less vegetation grows. When soil is covered with impervious material, such as concrete or asphalt, vegetation can't grow or decay, and its remains

become part of the soil. Similarly, when land is cleared of vegetation, less carbon is stored in the vegetation and below ground. Energy facilities cover land and reduce vegetation.

Estimates of the organic carbon stored in grassland and the soil under grassland are 1.15 kg-C/m^2 and 13.2 kg-C/m^2, respectively (Ni, 2002). Normally, when grass dies, the dead grass contributes to the soil organic carbon. The grass then regrows, removing carbon from the air by photosynthesis. If the soil is instead covered with concrete, the grass no longer exists to remove carbon from the air or store carbon in the soil. However, existing carbon stored underground remains. Some of this is oxidized, though, over time and carried away by ground water.

The carbon emissions due to developing land for an energy facility can be estimated simplistically by first summing the land areas covered by the facility; the mine where the fuel is extracted from (in the case of fossil fuels and uranium); the roads, railways, or pipelines needed to transport the fuel; and the waste disposal site associated with the facility. This summed area is then multiplied by the organic carbon content normally stored in vegetation per unit area that is lost plus the organic carbon content normally stored in soil under the vegetation per unit area that is lost. The latter value can be estimated as approximately one-third the original organic carbon content of the soil. The loss of carbon is then converted to a loss of carbon per unit electricity produced by the energy facility over a specified period of time. For purposes of Table 3.5, this period is 100 years. Example 3.8 provides an example calculation of CO_2e emissions from the covering land with an energy facility.

Example 3.8. Estimating the loss of carbon stored in vegetation and soil due to an energy facility.
Assume a 425 MW coal facility has a 65 percent capacity factor and has a footprint of 5.2 km^2, including the land for the coal facility, mining, railway transport, and waste disposal. Calculate the emission rate of CO_2 from the soil and vegetation, averaged over 100 years, due to this facility, assuming that it replaces grass and 34 percent of the soil carbon is lost.

Solution:
The energy generated over one year from this plant is 425 MW × 8760 h/y × 0.65 × 1,000 kW/MW = 2.42×10^9 kWh/y. Over 100 years, the energy produced is 2.42×10^{11} kWh.

The carbon lost in soil is 0.34 × 13.2 kg-C/m^2 = 4.5 kg-C/m^2 and that lost from vegetation is 1.15 kg-C/m^2, for a total of 5.64 kg-C/m^2. Multiplying by 1,000 g/kg and the molecular weight of CO_2 (44.0095 g-CO_2/mol), then dividing by the molecular weight of carbon (12.0107 g-C/mol) give 20,700 g-CO_2/m^2. Multiplying this by the land area covered by the facility and dividing by the 100-year energy use gives an emission rate from lost soil and vegetation carbon as 0.44g-CO_2/kWh, averaged over 100 years.

Because most of the carbon in soil and vegetation is lost immediately, the 100-year average loss of carbon from the soil provided in Table 3.5 underestimates the impact on climate damage of an energy facility that occupies land. Most climate impacts from the loss of carbon will begin when the emissions occur. Thus, for example, the impacts over 10 years of carbon loss in soil are 10 times those in Table 3.5. However, to maintain consistency with the other types of carbon-equivalent emissions in the table, that from soil carbon loss are also averaged over 100 years.

****

Table 1.2. *E*-folding lifetimes, 20-year GWPs, and 100-year GWPs of several global warming agents.

Chemical	*E*-folding lifetime	20-Year GWP	100-Year GWP
[a]CO_2	50-90 years	1	1

[b]BC+POC in fossil fuel soot	3-7 days	2,400-3,800	1,200-1,900
[b]BC+POC in biofuel soot	3-7 days	2,100-4,000	1,060-2,020
[c]CH_4	12.4 years	86	34
[c]N_2O	121 years	268	298
[c]$CFCl_3$ (CFC-11)	45 years	7,020	5,350
[d]CF_2Cl_2 (CFC-12)	100 years	10,200	10,800
[c]CF_4 (PFC-14)	50,000 years	4,950	7,350
[d]C_2F_6 (PFC-116)	10,000 years	8,210	11,100
[e]Tropospheric O_3	23 days	--	--
[f]NO_x-N	< 2 weeks	-560	-159
[g]SO_x-S	< 2 weeks	-1,400	-394

GWP=Global Warming Potential.

[a]The low-lifetime of CO_2 is the data-constrained lifetime upon increasing CO_2 emissions from Jacobson (2012a); the high-lifetime of CO_2 is calculated from Figure 9.6, which shows CO_2 decreasing by 65 ppmv (from 400 to 335 ppmv) over 65 years upon elimination of anthropogenic CO_2 emissions. Since the natural CO_2 is 275 ppmv, the anthropogenic CO_2 = 400-275=125 ppmv, and the lifetime of anthropogenic CO_2 is ~65 y / -ln((125-65) ppmv/125 ppmv) = ~90 years. The GWP of CO_2=1 by definition.

[b]POC is primary organic carbon co-emitted with black carbon from combustion sources. In the case of diesel exhaust, it is mostly lubricating oil and unburned fuel oil. In all cases, POC includes both absorbing organic (brown) carbon (BrC) and less absorbing organic carbon. Soot particles contain both BC and POC. The lifetime is from Jacobson (2012b) and the GWP is from Jacobson (2010a, Table 4), which accounts for direct effects, optical focusing effects, semi-direct effects, indirect effects, cloud absorption effects, and snow-albedo effects. The GWPs here are the surface temperature response after 20 or 100 years per unit continuous mass emissions (STRE) of BC+POC relative to the same for CO_2. STREs are analogous to GWPs (Jacobson, 2010a, Table 4 footnote).

[c]From Myhre et al. (2013) Table 8.7. Results from Etminan et al. (2016) suggest that the 20-y GWP of CH_4 may be up to 98.

[d]From Myhre et al. (2013) Table 8.A.1.

[e]From Myhre et al. (2013), Section 8.2.3.1. Tropospheric ozone is not emitted so does not have a GWP.

[f]From Myhre et al. (2013), Table 8.A.3, including aerosol direct and indirect effects. Values are on a per kg nitrogen basis.

[g]From Streets et al. (2001) and Jacobson (2002), including aerosol direct and indirect effects. Values are on a per kg sulfur basis. These numbers are STREs, which are analogous to GWPs (Footnote b).

References

ABB, HVDC-an ABB specialty, 2004, https://library.e.abb.com/public/d4863a9b0f77b74ec1257b0c00552758/HVDC%20Cable%20Transmission.pdf (accessed December 31, 2018).

ABB, HVDC technology for energy efficiency and grid reliability, 2005, https://www02.abb.com/global/abbzh/abbzh250.nsf/0/27c2fdbd96a879a4c12575ee00487a77/$file/HVDC+-+efficiency+and+reliability.pdf (accessed December 31, 2018).

ABC (American Bird Conservancy, American Bird Conservancy, https://abcbirds.org 2019 (accessed January 4, 2019).

AFDC, P., Public retail gas stations by year, 2014, https://afdc.energy.gov/data/10333, (accessed December 3, 2018).

Aghahosseini A, D. Bogdanov, and C. Breyer, A techno-economic study of an entirely renewable energy-based powers supply for North America for 2030 conditions, *Energies, 10*, 1171, doi:10.3390/en10081171, 2016.

Aghahosseini A., D. Bogdanov, L.S.N.S. Barbosa, and C. Breyer, Analyzing the feasibility of powering the Americas with renewable energy and inter-regional grid interconnections by 2030, *Renewable and Sustainable Energy Reviews, 105*, 187-205, 2019.

Allain, R., How much energy can you store in a stack of cement blocks, *Wired*, 2018, https://www.wired.com/story/battery-built-from-concrete/ (accessed April 10, 2019).

Allanore, A., L. Yin, and D. Sadoway, A new anode material for oxygen evolution in molten oxide electrolysis, *Nature, 497*, 353-356, 2013.

Allred, B.W., W.K. Smith, D. Twidwell, J.H. Haggerty, S.W. Running, D.E. Naugle, and S.D. Fuhlendorf, Ecosystem services lost to oil and gas in North America, *Science, 348*, 401-402, 2015.

Alcade, J., S. Flude, M. Wilkinson, G. Johnson, K. Edlmann, C.E. Bond, V. Scott, S.M.V. Gilfillan, X. Ogaya, and R.S. Haszeldine, Estimating geological CO2 storage security to deliver on climate mitigation, Nature *Communications, 9*, 2201, 2018.

Allen, M. R. *et al*., Warming caused by cumulative carbon emissions towards the trillionth tonne. Nature 458, 1163–1166, 2009.

Alvarez, R.A., D. Zavalao-Araiza, D.R. Lyon et al., Assessment of methane emissions from the U.S. oil and gas supply chain, *Science, 361*, 186-188, 2018.

Alvarez R.A., S.W. Pacala, J.J. Winebrake, W.L. Chameides, and S.P. Hamburg, Greater focus needed on methane leakage from natural gas infrastructure. *Proc*. *Nat*. *Acad*. *Sci*. doi: 10.1073/pnas.1202407109, 2012.

Archer, C.L., and M. Z. Jacobson, Spatial and temporal distributions of U.S. winds and wind power at 80 m derived from measurements, *J. Geophys. Res., 108* (D9) 4289, 2003.

Archer, C.L. and M.Z. Jacobson, Evaluation of global wind power, *J. Geophys. Res*., 110, D12110, doi:10.1029/2004JD005462, 2005.

Archer, C.L., and M.Z. Jacobson, Supplying baseload power and reducing transmission requirements by interconnecting wind farms, *J. Applied Meteorol. and Climatology*, 46, 1701-1717, doi:10.1175/2007JAMC1538.1, 2007.

Arcon/Sunmark, Large-scale showcase projects, 2017, http://arcon-sunmark.com/uploads/ARCON_References.pdf (accessed November 25, 2018).

Barber, H., Chapter 7, Electric heating fundamentals, In *The Efficient use of Energy*, 2nd edition, pp. 94-114, I.G.C. Dryden, ed., Butterworth-Heinemann, doi:10.1016/B978-0-408-01250-8.50016-7, 1982.

Barasa, M., D. Bogdanov, A.S. Oyewo, and C. Breyer, A cost optimal resolution for sub-Saharan Africa powered by 100% renewables in 2030, *Renewable and Sustainable Energy Reviews, 92*, 440-457, 2018.

Barbosa, L.S.N.S., D. Bogdanov, P. Vainikka, and C. Breyer, Hydro, wind, and solar power as a base for a 100% renewable energy supply for South and Central America, *PloS One*, doi:10.1371/journal.pone.0173820, 2017.

BBC News, Japan confirms first Fukushima worker death from radiation (2018) https://www.bbc.com/news/world-asia-45423575 (accessed June 9, 2019).

Becker, S., B.A. Frew, G.B. Andresen, T. Zeyer, S. Schramm, M. Greiner, and M.Z. Jacobson, Features of a fully renewable U.S. electricity-system: Optimized mixes of wind and solar PV and transmission grid

extensions, *Energy, 72*, 443-458, 2014.
Becker, S., B.A. Frew, G.B. Andresen, M.Z. Jacobson, S. Schramm, and M. Greiner, Renewable build-up pathways for the U.S.: Generation costs are not system costs, *Energy*, *81*, 437-445, 2015.
Bellevrat, E., and K West, Clean and efficient heat for industry, 2018, https://www.iea.org/newsroom/news/2018/january/commentary-clean-and-efficient-heat-for-industry.html (accessed November 17, 2018).
Berthelemy, M., and L.E. Rengel, Nuclear reactors' construction costs: The role of lead-time, standardization, and technological progress, *Energy Policy, 82*, 118-130, 2015.
Bistak, S., and S.Y. Kim, AC induction motors vs. permanent magnet synchronous motors, 2017, http://empoweringpumps.com/ac-induction-motors-versus-permanent-magnet-synchronous-motors-fuji/ (accessed January 5, 2018).
Bizee, Custom degree day data, 2019, http://www.degreedays.net, (accessed January 21, 2019).
Blakers, A., B. Lu, and M. Socks, 100% renewable electricity in Australia, *Energy, 133*, 471-482, 2017.
Blakers, A., B. Lu, M. Stocks, K. Anderson, and A. Nadolny, Pumped hydro storage to support 100% renewable power, Energy News, 36, 11-14, 2018.
Blakers, A., M. Stocks, B. Lu, C. Cheng, and A. Nadolny, Global pumped hydro atlas, 2019, http://re100.eng.anu.edu.au/global/ (accessed March 31, 2019).
Bloomberg NEF, A behind-the-scenes take on lithium-ion battery prices, 2019 https://about.bnef.com/blog/behind-scenes-take-lithium-ion-battery-prices/ (accessed June 28, 2019).
Boden, T., B. Andres, and G. Marland, Global CO_2 emissions from fossil-fuel burning, cement manufacture, and gas flaring: 1751-2011, 2011, http://cdiac.ornl.gov/ftp/ndp030/global.1751_2011.ems (accessed January 24, 2019).
Boeing, 747-8 Airplane characteristics for airport planning, 2012, http://www.boeing.com/assets/pdf/commercial/airports/acaps/747_8.pdf (accessed March 27, 2019).
Bogdanov, D., and C. Breyer, North-east Asian super grid for 100% renewable energy supply: Optimal mix of energy technologies for electricity, gas, and heat supply options, *Energy Conversion and Management, 112*, 176-190, 2016.
Bogdanov, D., J. Farfan, K. Sadovskaia, A. Aghahosseini, M. Child, A. Gulagi, A.S. Oyewo, L.S.N.S. Barbosa, and C. Breyer, Radical transformation pathway towards sustainable electricity via evolutionary steps, *Nature Communications, 10,* 1077, doi: 10.1038/s41467-019-08855-1, 2019.
Boiocchi, R., K.V. Gemaey, and G. Sin, Control of wastewater N2O emission by balancing the microbial communities using a fuzzy-logic approach, *IFAC-PapersOnLine, 49*, 1157-1162, 206.
Bond, T.C., D.G. Streets, K.F. Yarber, S.M. Nelson, J.-H. Woo, and Z. Klimont, A technology-based global emission inventory of black and organic carbon emissions from combustion, *J. Geophys. Res., 109*, D14203, doi:10.1029/2003JD003697, 2004.
Bond, T.C., and Bond, T.C., S.J. Doherty, D.W. Fahey, P.M. Forster, T. Berntsen, O. Boucher, B.J. DeAngelo, M.G. Flanner, S. Ghan, B. Karcher, D. Koch, S. Kinne, Y. Kondo, P.K. Quinn, M.C. Sarofim, M.G. Schultz, M. Schulz, C. Venkataraman, H. Zhang, S. Zhang, N. Bellouin, S.K. Guttikunda, P.K. Hopke, M.Z. Jacobson, J.W. Kaiser, Z. Klimont, U. Lohmann, J.P. Schwarz, D. Shindell, T. Storelvmo, S.G. Warren and C.S. Zender, Bounding the role of black carbon in the climate system: A scientific assessment, *J. Geophys. Res*., *118*, 5380-5552, doi: 10.1002/jgrd.50171, 2013Jacobson, M. Z., Isolating nitrated and aromatic aerosols and nitrated aromatic gases as sources of ultraviolet light absorption, *J. Geophys. Res., 104*, 3527-3542, 1999.
Boukhalf, S., and N. Kaul, 10 disruptive battery technologies trying to compete with lithium-ion, 2019, https://www.solarpowerworldonline.com/2019/01/10-disruptive-battery-technologies-trying-to-compete-with-lithium-ion/ (accessed February 2, 2019).
Boyer, G., Appalachian power rolls out 100% renewable option for customers, WFXR News, 2019, https://www.wfxrtv.com/news/appalachian-power-rolls-out-100-renewable-option-for-va-customers/ (accessed August 21, 2019).
Bremner, S.P., M.Y. Levy, and C.B. Honsberg, Analysis of tandem solar cell efficiencies under {AM1.5G} spectrum using a rapid flux calculation method, Progress in Photovoltaics: Research and Applications, 16, 225-233, 2008.
Breyer, C., Economics of hybrid photovoltaic power plants, Pro Business ISBN: 978-3863863906, 2012.

Breyer, C., D. Bogdanov, A. Gulagi, A. Aghahossein, L.S.N.S. Barbosa, O. Koskinen, M. Barasa, U. Caldera, S. Afanasyeva, M. Child, J. Farfan and P. Vainikka, On the role of solar photovoltaics in global energy transition scenarios, Prog. Photovolt. Res. Appl. 25, 727-745, 2017.

British Petroleum, BP statistical review of world energy, 2018, https://www.bp.com/content/dam/bp/business-sites/en/global/corporate/pdfs/energy-economics/statistical-review/bp-stats-review-2018-co2-emissions.pdf (accessed December 15, 2018).

Brown, T.W., T. Bischof-Niemz, K. Blok, C. Breyer, H. Lund, and B.V. Mathiesen, Response to 'Burden of proof: A comprehensive review of the feasibility of 100% renewable electricity systems,' *Renewable and Sustainable Energy Reviews, 92*, 834-847, 2018.

Bruckner T., I.A. Bashmakov, Y. Mulugetta, H. Chum, A. de la Vega Navarro, J. Edmonds, A. Faaij, B. Fungtammasan, A. Garg, E. Hertwich, D. Honnery, D. Infield, M. Kainuma, S. Khennas, S. Kim, H.B. Nimir, K. Riahi, N. Strachan, R. Wiser, and X. Zhang, Energy Systems. In: *Climate Change 2014: Mitigation of Climate Change. Contribution of Working Group III to the Fifth Assessment Report of the Intergovernmental Panel on Climate Change* [Edenhofer, O., R. Pichs-Madruga, Y. Sokona, E. Farahani, S. Kadner, K. Seyboth, A. Adler, I. Baum, S. Brunner, P. Eickemeier, B. Kriemann, J. Savolainen, S. Schlömer, C. von Stechow, T. Zwickel and J.C. Minx (eds.)]. Cambridge University Press, Cambridge, United Kingdom and New York, NY, USA, 2014.

BTS (Bureau of Transportation Statistics), U.S. oil and gas pipeline mileage, 2018, https://www.bts.gov/content/us-oil-and-gas-pipeline-mileage (accessed December 3, 2018).

Budischak, C., D. Sewell, H. Thompson, L. Mach, D.E. Veron, and W. Kempton, Cost-minimized combinations of wind power, solar power, and electrochemical storage, powering the grid up to 99.9% of the time, *J Power Sources, 225*, 60-74, 2013.

Build Abroad, Ferrock: A stronger, more flexible and greener alternative to concrete, 2016, https://buildabroad.org/2016/09/27/ferrock/ (accessed November 20, 2018).

Burke, M., S.M. Hsiang, and E. Miguel, Global non-linear effect of temperature on economic production, *Nature*, *527*, 235-239, 2015.

Burnett, R., Global estimates of mortality associated with long-term exposure to outdoor fine particulate matter, *Proc. Natl. Acad. Sci., 115*, 9592-9597, 2018.

Business Dictionary, Installed capacity: definition, 2019 http://www.businessdictionary.com/definition/installed-capacity.html (accessed March 15, 2019).

CARB (California Air Resources Board), Estimate of premature deaths associated with fine particle pollution ($PM_{2.5}$) in California using a U.S. Environmental Protection Agency Methodology, 2010, https://www.arb.ca.gov/research/health/pm-mort/pm-report_2010.pdf (accessed January 15, 2019).

Caldera, U., and C. Breyer, Role that battery and water storage play in Saudi Arabia's transition to an integrated 100% renewable energy power system, J. Energy Storage, 17, 299-310, 2018.

California Senate, SB 100 FAQs, 2018, https://focus.senate.ca.gov/sb100/faqs (accessed February 6, 2019).

Carbon Cure, Carbon Cure, 2018, https://www.carboncure.com (accessed November 20, 2018).

CDC (Center for Disease Control and Prevention), Research on long-term exposure: Uranium miners, 2000, https://www.cdc.gov/niosh/pgms/worknotify/uranium.html (accessed December 9, 2018).

Cebulla, F., and M.Z. Jacobson, Alternative renewable energy scenarios for New York, *Journal of Cleaner Production*, *205*, 884-894, 2018.

Chakratek, Flywheel specifications and comparison, 2019, https://www.chakratec.com/technology/ (accessed March 18, 2019).

Chang, T.P., The Sun's apparent position and the optimal tilt angle of a solar collector in the northern hemisphere, *Solar Energy 83*, 1274-1284, 2009.

Child, M., and C. Breyer, Vision and initial feasibility analysis of a decarbonized Finnish energy system for 2050. *Renewable and Sustainable Energy Reviews, 66*, 517-536, 2016.

Child, M., A. Nordling, and C. Breyer, The impacts of high V2G participation in a 100% renewable Aland energy system, Energies, 11, 2206, https://doi.org/10.3390/en11092206, 2018.

CEC (California Energy Commission), A review of transmission losses in planning studies, 2011, https://www.energy.ca.gov/2011publications/CEC-200-2011-009/CEC-200-2011-009.pdf (accessed December 31, 2018).

Climate Group, EV100 members, 2019, https://www.theclimategroup.org/ev100-members (accessed September 22, 2019).

Clinton, H., Hillary is ready for 100, October 16, 2015, http://www.c-span.org/video/?c4557641/hillary-readyfor100 (Accessed February 7, 2019).

Cockburn, H., Scotland generating enough wind energy to power two Scotlands, 2019, https://www.independent.co.uk/environment/scotland-wind-power-on-shore-renewable-energy-climate-change-uk-a9013066.html (accessed July 26, 2019).

Colella, W.G., M.Z. Jacobson, and D.M. Golden, Switching to a U.S. hydrogen fuel cell vehicle fleet: The resultant change in emissions, energy use, and global warming gases, *J. Power Sources*, *150*, 150-181, 2005.

Connolly, D., H. Lund, B.V. Mathiesen, and M. Leahy, The first step to a 100% renewable energy-system for Ireland, Applied Energy, 88, 502-507, 2011.

Connolly, D., and B.V. Mathiesen, Technical and economic analysis of one potential pathway to a 100% renewable energy system, *Intl. J. Sustainable Energy Planning & Management, 1,* 7-28, 2014.

Connolly, D., H. Lund, and B.V. Mathiesen, Smart energy Europe: The technical and economic impact of one potential 100% renewable energy scenario for the European Union, *Renewable and Sustainable Energy Reviews, 60,* 1634-1653, 2016.

Consumer Reports, Electric lawn mowers that rival gas models, 2017, https://www.consumerreports.org/push-mowers/electric-lawn-mowers-that-rival-gas-models/ (accessed November 21, 2018).

Corcoran, B.A., N. Jenkins, and M.Z. Jacobson, Effects of aggregating electric load in the United States. *Energy Policy*, *46*, 399-416, 2012.

Cornell University, How lake source cooling works, 2019, https://energyandsustainability.fs.cornell.edu/util/cooling/production/lsc/works.cfm (accessed May 1, 2019).

Crossley, I, Simplifying and lightening offshore turbines with compressed air energy storage, Wind Power, 2018, https://www.windpoweroffshore.com/article/1463030/simplifying-lightening-offshore-turbines-compressed-air-energy-storage (accessed March 18, 2019).

Czisch, G., PhD Dissertation, University of Kassel, 2005, https://kobra.uni-kassel.de/handle/123456789/200604119596 (accessed February 24, 2019).

Czisch, G., and G. Giebel, Realisable scenarios for a future electricity supplies based 100% on renewable energies, Riso-R-1608 (EN), 2007.

Damkjaer, L., Gram Fjernvarme 2016, 2016, https://www.youtube.com/watch?v=PdF8e1t7St8 (accessed November 25, 2018).

Dandelion, Geothermal heating and air conditioning is so efficient, it pays for itself, https://dandelionenergy.com, 2018 (accessed November 17, 2018).

De Coninck, H., A. Revi, M. Babiker, P. Bertoldi, M. Buckeridge, A. Cartwright, W. Dong, J. Ford, S. Fuss, J.-C. Hourcade, D. Ley, R. Mechler, P. Newman, A. Revokatova, S. Schultz, L. Steg, and T. Sugiyama, Chapter 4: Strengthening and implementing the global response, in Intergovernmental Panel on Climate Change, Global Warming of 1.5 ^{o}C report, 2018.

De Gouw, J.A., D.D. Parrish, G.J. Frost, and M. Trainer, Reduced emissions of CO_2, NO_x, and SO_2 from U.S. power plants owing to switch from coal to natural gas with combined cycle technology, *Earth's Future, 2,* 75-82, 2014.

De Gracia, A., and L.F. Cabeza, Phase change materials and thermal energy storage for buildings, *Energy and Buildings, 103*, 414-419, 2015.

Delucchi, M, A conceptual framework for estimating the climate impacts of land-use change due to energy crop programs, *Biomass and Bioenergy*, *35*, 2337-2360, 2011.

Delucchi, M.Z., and M.Z. Jacobson, Providing all global energy with wind, water, and solar power, Part II: Reliability, System and Transmission Costs, and Policies, *Energy Policy*, 39, 1170-1190, doi:10.1016/j.enpol.2010.11.045, 2011.

Denholm, P., Y.-H. Wan, M. Hummon, and M. Mehos, The value of CSP with thermal energy storage in the western United States, *Energy Procedia, 49*, 1622-1631, 2014.

Denyer, S., Eight years after Fukushima's meltdown, the land is recovering, but public trust is not, Washington Post, 2019, https://www.washingtonpost.com/world/asia_pacific/eight-years-after-fukushimas-meltdown-the-land-is-recovering-but-public-trust-has-not/2019/02/19/0bb29756-255d-11e9-b5b4-1d18dfb7b084_story.html?utm_term=.8344c816d5bb (accessed December 21, 2019).

De Stercke, S., Dynamics of Energy Systems: a Useful Perspective. IIASA Interim Report No. IR-14-013, International Institute for Applied Systems Analysis, IIASA, Laxenburg, Austria, 2014.

Diesendorf, M., and B. Elliston, The feasibility of 100% renewable electricity systems: A response to critics, *Renewable and Sustainable Energy Reviews, 93*, 318-330, 2018.

DOE (U.S. Department of Energy), 2014: The year of concentrating solar power, 2014, https://www.energy.gov/sites/prod/files/2014/05/f15/2014_csp_report.pdf (accessed March 30, 2019).

DOE (U.S. Department of Energy), Fuel Cells, 2015, https://www.energy.gov/sites/prod/files/2015/11/f27/fcto_fuel_cells_fact_sheet.pdf (accessed January 11, 2019).

DOE (U.S. Department of Energy), Quadrennial Technology Review, Chapter 6: Innovative clean energy technologies in advanced manufacturing: Technology assessment, 2015, https://www.energy.gov/sites/prod/files/2016/06/f32/QTR2015-6I-Process-Heating.pdf (accessed Nov. 17, 2018).

DOE (U.S. Department of Energy), How do wind turbines work? 2019, https://www.energy.gov/eere/wind/wind-energy-technologies-office (accessed March 27, 2019).

DPC (U.S. Democratic Platform Committee), 2016 Democratic Party Platform, July 9, 2016, https://democrats.org/wp-content/uploads/2018/10/2016_DNC_Platform.pdf (Accessed February 7, 2019)

Douglas, C.A., G.P. Harrison, and J.P. Chick, Life cycle assessment of the Seagen marine current turbine, *Proc. Inst. Mech. Eng. Part M: J of Engineering for the Maritime Environment, 222*, 1-12, 2008.

Drake Landing, Drake Landing Solar Community, 2016, https://www.dlsc.ca/how.htm (accessed March 26, 2019).

Drupp, M., Freeman, M., Groom, B., and Nesje, F., *Discounting disentangled: an expert survey on the determinants of the long-term social discount rate* The Centre for Climate Change Economics and Policy Working Paper No. 195 and Grantham Research Institute on Climate Change and the Environment Working Paper No. 172 (CCCEP and Grantham Research Institute), 2015.

Duan, Y., and D.C. Sorescu, CO_2 capture properties of alkaline earth metal oxides and hydroxides: A combined density functional theory and lattice phonom dynamics study, J. Chem. Phys., 133, 074508, 2010.

Duke Energy, More renewable energy options available under Duke Energy's Green Source Advantage, 2019, https://news.duke-energy.com/releases/more-renewable-energy-options-available-under-duke-energys-green-source-advantage?_ga=2.88266651.1875174277.1566405614-658711925.1566405614 (accessed August 21, 2019).

Dvorak, M., C.L. Archer, and M.Z. Jacobson, California offshore wind energy potential, *Renewable Energy*, 35, 1244-1254, doi:10.1016/j.renene.2009.11.022, 2010.

Dvorak, M.J., E.D. Stoutenburg, C.L. Archer, W. Kempton, and M.Z. Jacobson, Where is the ideal location for a U.S. East Coast offshore grid, *Geophys. Res. Lett*., *39*, L06804, doi:10.1029/2011GL050659, 2012.

Dvorak, M.J., B.A. Corcoran, J.E. Ten Hoeve, N.G. McIntyre, and M.Z. Jacobson, U.S. East Coast offshore wind energy resources and their relationship to peak-time electricity demand, *Wind Energy*, 16, 977-997, doi:10.1002/we.1524, 2013.

Earthworks, Responsible minerals sourcing for renewable energy, 2019, https://earthworks.org/publications/responsible-minerals-sourcing-for-renewable-energy/ (accessed May 1, 2019).

Eddington S.A., On the radiative equilibrium of the stars, *Mon. Not. Roy. Astronom. Soc*., *77*, 16-35, 1916.

EIA (Energy Information Administration, U.S.) (2016). *International Energy Outlook 2016* DOE/EIA-0484, 2016, http://www.eia.gov/forecasts/ieo/pdf/0484(2016).pdf, https://www.eia.gov/forecasts/ieo/, http://www.eia.gov/forecasts/ieo/ieo_tables.cfm (accessed January 10, 2019).

EIA (U.S. Energy Information Administration), Hydraulically fractured wells provide two-thirds of U.S. natural gas production, 2016, https://www.eia.gov/todayinenergy/detail.php?id=26112 (accessed December 2, 2018).

EIA (U.S. Energy Information Administration), Today in energy, 2017, https://www.eia.gov/todayinenergy/detail.php?id=33552 (accessed December 4, 2018).

EIA (U.S. Energy Information Administration), Table 1. Coal production and number of mines by state and mine type, 2017 and 2016, 2018a, https://www.eia.gov/coal/annual/pdf/table1.pdf (accessed December 3, 2018).
EIA (U.S. Energy Information Administration), Frequently asked questions, 2018b, https://www.eia.gov/tools/faqs/faq.php?id=29&t=6 (accessed December 3, 2018).
EIA (U.S. Energy Information Administration), Table 4.1. Count of electric power industry power plants by sector, by predominant energy sources within plant, 2007 through 2017, 2018c, https://www.eia.gov/electricity/annual/html/epa_04_01.html (accessed December 3, 2018).
EIA (U.S. Energy Information Administration), Table 1.1. Total electric power industry summary statistics, 2017 and 2016, 2018d, https://www.eia.gov/electricity/annual/html/epa_01_01.html (accessed December 5, 2018).
EIA (Energy Information Administration), How much electricity is lost in transmission and distribution in the United States, 2018e, https://www.eia.gov/tools/faqs/faq.php?id=105&t=3 (accessed December 31, 2018).
Electrical Systems, Principle of electricity generation, 2019, http://www.skm-eleksys.com/2010/02/practical-power-system.html (accessed April 5, 2019).
Electronics Hub, Characteristics and working of P-N junction diode, 2015, https://www.electronicshub.org/characteristics-and-working-of-p-n-junction-diode/ (accessed March 31, 2019).
Electronics Tutorials, Capacitor tutorial summary, 2019a, https://www.electronics-tutorials.ws/capacitor/cap_9.html (accessed April 3, 2019).
Electronics Tutorials, Reactive power, 2019b, https://www.electronics-tutorials.ws/accircuits/reactive-power.html (accessed April 3, 2019).
ELI (Environmental Law Institute), Estimating U.S. government subsidies to energy sources: 2002-2008, 2009, https://www.eli.org/research-report/estimating-us-government-subsidies-energy-sources-2002-2008 (accessed January 25, 2019).
Elliston, B., M. Diesendorf, and I. MacGill, Simulations of scenarios with 100% renewable electricity in the Australian National Electricity Market, *Energy Policy, 45*, 606-613, 2012.
Elliston, B., I. MacGill, and M. Diesendorf, Least cost 100% renewable electricity scenarios in the Australian National Electricity Market, *Energy Policy, 59*, 270-282, 2013.
Elliston, B., I. MacGill, and M. Diesendorf, Comparing least cost scenarios for 100% renewable electricity with low emission fossil fuel scenarios in the Australian National Electricity Market, *Renew Energy, 66,* 196-204, 2014.
Enevoldsen, P., and M.Z. Jacobson, Data investigation of installed and output power densities of onshore and offshore wind turbines worldwide, *Wind Energy*, 2020.
ENTSO-E (European Network of Transmission System Operators for Electricity), European load data, 2016, https://www.entsoe.eu/db-query/country-packages/production-consumption-exchange-package, 2016 (accessed January 29, 2019).
Erlich, I., and M. Wilch, Frequency control by wind turbines, IEEE PES General Meeting, July 25-29, 2010, doi: 10.1109/PES.2010.5589911, https://ieeexplore.ieee.org/document/5589911 (accessed March 2, 2019).
Esteban, M., J. Portugal-Pereira, B.C. Mclellan, J. Bricker, H. Farzaneh, N. Djalikova, K.N. Ishihara, H. Takagi, and V. Roeber, 100% renewable energy system in Japan: Smoothening and ancillary services, *Applied Energy*, 224, 698-707, 2018.
Etminan, M., G. Myhre, E.J. Highwood, and K.P. Shine, Radiative forcing of carbon dioxide, methane, and nitrous oxide: A significant revision of the methane radiative forcing, *Geophys. Res. Lett., 43*, 12614-12623, 2016.
European Commission, EDGAR: Emissions database for global atmospheric research, 2019, https://edgar.jrc.ec.europa.eu/background.php (accessed May 26, 2019).
Evarts, E.C., The world's largest EV never has to be recharged, Green Car Reports, 2019, https://www.greencarreports.com/news/1124478_world-s-largest-ev-never-has-to-be-recharged (accessed August 20, 2019).

EVWind, Current status of concentrated solar power globally, 2018, https://www.evwind.es/2018/07/25/current-status-of-concentrated-solar-power-csp-globally/64041 (accessed January 9, 2019).

Faulstich, S., B. Hahn, and P.J. Tavner, Wind turbine downtime and its importance for offshore deployment, *Wind Energy, 14*, 327-337, 2011.

Feng, Z., Stationary high-pressure hydrogen storage, 2018, https://www.energy.gov/sites/prod/files/2014/03/f10/csd_workshop_7_feng.pdf (accessed November 28, 2018).

FERC (Federal Energy Regulatory Commission), Current state of and issues concerning underground natural gas storage, 2004, https://www.ferc.gov/EventCalendar/Files/20041020081349-final-gs-report.pdf (accessed December 3, 2018).

Fetter, S., How long will the world's uranium supplies last, *Scientific American, 9*, 2009.

Fischer, D., and H. Madani, On heat pumps in smart grids: A review. *Renewable and Sustainable Energy Reviews*, *70*, 342-357, 2017.

Flury, K., and R. Frischknecht, Lifecycle inventories of hydroelectric power generation, 2012, ESU Services, http://esu-services.ch/fileadmin/download/publicLCI/flury-2012-hydroelectric-power-generation.pdf (accessed December 8, 2018).

Frangoul, A., Scandinavia's biggest offshore wind farm is officially open, 2019, https://www.cnbc.com/2019/08/23/scandinavias-biggest-offshore-wind-farm-is-officially-open.html?__source=sharebar%7Ctwitter&par=sharebar (accessed August 23, 2019).

Free Dictionary, Installed capacity: definition, 2019 https://encyclopedia2.thefreedictionary.com/Installed+Capacity (accessed March 15, 2019).

Frew, B.A., S. Becker, M.J. Dvorak, G.B. Andresen, and M.Z. Jacobson, Flexibility mechanisms and pathways to a highly renewable U.S. electricity future, *Energy*, *101*, 65-78, 2016.

Frew, B.A., and M.Z. Jacobson, Temporal and spatial tradeoffs in power system modeling with assumptions about storage: An application of the POWER model, *Energy*, 117, 198-213, 2016.

Friedlingstein P., R.M. Andrew, J. Rogelj, G.P. Peters, J.G. Canadell, R. Knutti, G.L. Luderer, M.R. Raupach, M. Schaeffer, D.P. van Vuuren, and C. Le Quere, Persistent growth of CO_2 emissions and implications for reaching climate targets. *Nature Geoscience* 7: 709–715, 2014.

Fthenakis, V., and M. Raugei, Environmental life-cycle assessment of photovoltaic systems, in *The Performance of Photovoltaic (PV) Systems: Modelling, Measurement, and Assessment*, N. Pearsall, Ed., pp. 209-232, 2017.

Fuhrmann, M., Spreading temptation: Proliferation and peaceful nuclear cooperation agreements (March 9, 2009). International Security, Vol. 34, No. 1, Summer 2009. Available at SSRN: https://ssrn.com/abstract=1356091 (accessed September 9, 2019).

Gaine K, and A. Duffy, A life cycle cost analysis of large-scale thermal energy storage for buildings using combined heat and power, *Zero Emission Buildings Conference Proceedings*, eds Haase M, Andresen I, Hestnes A (Trondheim, Norway), 7-8 June 2010.

Garthwaite, J., What should we do with nuclear waste, Stanford Earth, 2018, https://earth.stanford.edu/news/qa-what-should-we-do-nuclear-waste#gs.1sfx0x (accessed March 20, 2019).

GBD (Global Burden of Disease 2013 Risk Factors Collaborators), Global, regional, and national comparative risk assessment of 79 behavioral, environmental and occupational, and metabolic risks or clusters of risks in 188 countries, 1990-2013: a systematic analysis for the Global Burden of Disease Study 2013, *Lancet, 386*, 2287-2323, 2015.

GE (General Electric), Haliade-X offshore wind turbine platform, https://www.ge.com/renewableenergy/wind-energy/turbines/haliade-x-offshore-turbine, 2018 (accessed November 16, 2018).

Gerber H., Y. Takano, T.J. Garrett, and P.V. Hobbs, Nephelometer measurements of the asymmetry parameter, volume extinction coefficient, and backscatter ratio in Arctic clouds, *J. Atmos. Sci*., *57*, 3021-3033, 2000.

Geuss, M., Florida utility to close natural gas plants, build massive solar-powered battery, Ars Technica, 2019, https://arstechnica.com/information-technology/2019/03/florida-utility-to-close-natural-gas-plants-build-massive-solar-powered-battery/ (accessed April 1, 2019).

GHD, Cassada wind farm decommissioning cost estimate, 2017, http://www.charlotteny.org/pdfs/2018/wind/11110309-RPT1%20FINAL%20%207-11-2017.pdf (accessed January 16, 2019).

Ginnebaugh, D.L., J. Liang, and M.Z. Jacobson, Examining the temperature dependence of ethanol (E85) versus gasoline emissions on air pollution with a largely-explicit chemical mechanism**,** *Atmos. Environ., 44,* 1192-1199, doi:10.1016/j.atmosenv.2009.12.024, 2010.

Ginnebaugh, D.L., and M.Z. Jacobson, Examining the impacts of ethanol (E85) versus gasoline photochemical production of smog in a fog using near-explicit gas- and aqueous-chemistry mechanisms, *Environmental Research Letters*, 7, 045901, doi:10.1088/1748-9326/7/4/045901, 2012.

Green Party US, Green New Deal – Full Language, 2018, https://www.gp.org/gnd_full (accessed September 16, 2019).

Gross, B., Efficiency of gravitational mass storage system, 2019, https://twitter.com/Bill_Gross/status/1164617097927806976/photo/1 (accessed August 22, 2019).

Gulagi, A., D. Bogdanov, and C. Breyer, A cost optimized fully sustainable power system for Southeast Asia and the Pacific Rim, *Energies, 10*, 583, doi:10.3390/en10050583, 2017a.

Gulagi, A. P. Choudhary, D. Bogdanov, and C. Breyer, Electricity system based on 100% renewable for India and SAARC, *PLoS ONE*, doi:10.1371/journal.pone.0180611, 2017b.

Hampson, S. E., J. A. Andres, M. E. Lee, L. S. Foster, R. E. Glasgow, and E. Lichtenstein, Lay understanding of synergistic risk: the case of radon and cigarette smoking, *Risk Analysis*, *18*, 343-350, 1998.

Hanley, S., Energy Vault proposes and energy storage system using concrete blocks, Cleantechnica, 2018, https://cleantechnica.com/2018/08/21/energy-vault-proposes-an-energy-storage-system-using-concrete-blocks/ (accessed April 10, 2019).

Hansen, K., B. Mathiessen, and I.R. Skov, Full energy system transition towards 100% renewable energy in Germany in 2050, *Renewable and Sustainable Energy Reviews, 102*, 1-13, 2019a.

Hansen, K., C. Breyer, and H. Lund, Status and perspectives on 100% renewable energy systems, *Energy, 175*, 471-480, 2019b.

Harrabin, R., How liquid air could help keep the lights on, BBC News, 2019, https://www.bbc.com/news/business-50140110 (accessed October 30, 2019).

Hart, E.K., and M.Z. Jacobson, A Monte Carlo approach to generator portfolio planning and carbon emissions assessments of systems with large penetrations of variable renewables, *Renewable Energy*, *36*, 2278-2286, doi:10.1016/j.renene.2011.01.015, 2011.

Hart, E.K., E.D. Stoutenburg, and M.Z. Jacobson, The potential of intermittent renewables to meet electric power demand: A review of current analytical techniques, *Proceedings of the IEEE*, *100*, 322-334, doi:10.1109/JPROC.2011.2144951, 2012.

Hart, E.K., and M.Z. Jacobson, The carbon abatement potential of high penetration intermittent renewables, *Energy and Environmental Science*, *5*, 6592-6601, doi:10.1039/C2EE03490E, 2012.

Harvey, L.D.D., Resource implications of alternative strategies for achieving zero greenhouse gas emissions from light-duty vehicles by 2060, *Applied Energy, 212*, 663-679.

Hasager, C.B., L. Rasmussen, A. Pena, L.E. Jensen, and P.-E. Rethore, Wind farm wake: the Horns Rev photo case, *Energies, 6*, 696-716, 2013.

Henshaw, D. L., J. P. Eatough, and R. B. Richardson, Radon as a causative factor in induction of myeloid leukaemia and other cancers, *Lancet*, *335*, 1008-1012, 1990.

Hoste, G.R.G., M.J. Dvorak, and M.Z. Jacobson, Matching hourly and peak demand by combining different renewable energy sources, Stanford University Technical Report, 2009, https://web.stanford.edu/group/efmh/jacobson/Articles/I/CombiningRenew/HosteFinalDraft (accessed January 27, 2019).

Hou, P., P. Enevoldsen, J. Eichman, W. Hu, M.Z. Jacobson, and Z. Chen, Optimizing investments in coupled offshore wind-electrolytic hydrogen storage systems in Denmark, *J. Power Sources, 359*, 186-197, doi:10.1016/j.jpowsour.2017.05.048, 2017.

Houghton, R.A., Annual net flux of carbon to the atmosphere from land-use change: 1850-2005, 2015, http://cdiac.ornl.gov/trends/landuse/houghton/1850-2005.txt (accessed January 24, 2019).
House (U.S. House of Representatives), H.Res.540, 2015, https://www.congress.gov/bill/114th-congress/house-resolution/540/text (accessed February 7, 2019).
House (U.S. House of Representatives), H.R.3314 – 100 by '50 Act, 2017a, "https://www.congress.gov/bill/115th-congress/house-bill/3314 (accessed February 7, 2019).
House (U.S. House of Representatives), H.R.3671 – Off Fossil Fuels For A Better Future Act, 2017b, "https://www.congress.gov/bill/115th-congress/house-bill/3671/text (accessed February 7, 2019).
House (U.S. House of Representatives), H.R. 330 – Climate Solutions Act of 2019, 2019a, https://www.congress.gov/bill/116th-congress/house-bill/330/text (accessed February 7, 2019).
House (U.S. House of Representatives), Resolution recognizing the duty of the federal government to create a green new deal, 2019b, https://www.congress.gov/bill/116th-congress/house-resolution/109 https://apps.npr.org/documents/document.html?id=5729035-Green-New-Deal-FAQ (accessed February 10, 2019).
Howarth, R.W., A bridge to nowhere: methane emissions and the greenhouse gas footprint of natural gas, *Energy Science & Engineering*, *2*, 47-60, 2014.
Howarth, R.W., Is shale gas a major driver of recent increase in global atmospheric methane, *Biogeosciences 16*, 3033-3046, 2019.
Howarth, R.W., R. Santoro, and A. Ingraffea, Methane and the greenhouse gas footprint of natural gas from shale formations, *Climatic Change, 106*, 679-690, 2011.
Howarth, R.W., R. Santoro, and A. Ingraffea, Venting and leaking of methane from shale gas development: response to Cathles et al., Climatic Change, 2012.
HSMag, Simulation permanent magnet generators, 2016, https://www.hsmagnets.com/blog/simulation-permanent-magnet-generators/ (accessed July 23, 2019)
Hu, S-y, and J.-h Cheng, Performance evaluation of pairing between sites and wind turbines, *Renewable Energy, 32,* 1934-1947. 2007.
Hulls, P.J., Development of the industrial use of dielectric heating in the United Kingdom, J. Microwave Power, 17, 28-38, 2016.
Hunt, J.D., B. Zakeri, G. Falchetta, A. Nascimento, Y. Wada, and K. Riahi, Mountain gravity energy storage: A new solution for closing the gap between existing short- and long-term storage technologies, Energy, doi:10.1016/j.energy.2019.116419, 2019.
ICF Consulting, Life cycle greenhouse gas emissions of natural gas, 2012, https://www.capp.ca/-/media/capp/customer-portal/documents/215278.pdf (accessed January 22, 2019).
IEA (International Energy Agency), Integrated cost-effective large-scale thermal energy storage for smart district heating and cooling, 2018a, https://www.iea-dhc.org/fileadmin/documents/Annex_XII/IEA_DHC_AXII_Design_Aspects_for_Large_Scale_ATES_PTES_draft.pdf (accessed November 25, 2018).
IEA (International Energy Agency), Wind energy, 2018b https://www.iea.org/topics/renewables/wind/ (accessed January 9, 2019).
IEA (International Energy Agency), Geothermal energy, 2018c https://www.iea.org/topics/renewables/geothermal/ (accessed January 9, 2019).
IEA (International Energy Agency), Solar PV, 2018d https://www.iea.org/tcep/power/renewables/solar/ (accessed January 9, 2019).
IEA (International Energy Agency), *Statistics*, 2019, https://www.iea.org/statistics/ (accessed January 5, 2019).
IEC (International Electrotechnical Commission), Efficient electrical energy transmission and distribution, 2007, https://basecamp.iec.ch/download/efficient-electrical-energy-transmission-and-distribution/ (accessed December 31, 2018).
IGU (International Gas Union), Natural gas conversion guide, 2018, http://agnatural.pt/documentos/ver/natural-gas-conversion-guide_cb4f0ccd80ccaf88ca5ec336a38600867db5aaf1.pdf (accessed December 2, 2018).
IHA (International Hydropower Association), 2018 hydropower status report, 2018, https://www.hydropower.org/publications/2018-hydropower-status-report (accessed January 9, 2019).

IPCC (Intergovermental Panel on Climate Change), *Special Report on Emission Scenarios (SRES) final data*, 2000, http://sres.ciesin.org/final_data.html (accessed January 23, 2019).

IPCC (Intergovernmental Panel on Climate Change), *IPCC special report on carbon dioxide capture and storage*. Prepared by working group III, Metz. B., O. Davidson, H. C. de Coninck, M. Loos, and L.A. Meyer (eds.). Cambridge University Press, Cambridge, United Kingdom and New York, NY, USA, 442 pp. http://arch.rivm.nl/env/int/ipcc/, 2005 (accessed June 26, 2019).

IPCC (Intergovernmental Panel on Climate Change), *Special report: Global warming of 1.5º*, 2018, https://www.ipcc.ch/sr15/ (accessed June 26, 2019).

IranWatch, Iran's nuclear potential before the implementation of the nuclear agreement, 2015, https://www.iranwatch.org/our-publications/articles-reports/irans-nuclear-timetable (accessed December 9, 2018).

IRENA (International Renewable Energy Agency), Thermal energy storage. IEA-ETSAP and IRENA Technology Brief E17, IRENA, Abu Dhabi, 2013.

Jacobson M. Z., *Developing, coupling, and applying a gas, aerosol, transport, and radiation model to study urban and regional air pollution*. Ph.D. Dissertation, Dept. of Atmospheric Sciences, University of California, Los Angeles, 436 pp, 1994.

Jacobson, M. Z., R. Lu, R. P. Turco, and O. B. Toon, Development and application of a new air pollution modeling system. Part I: Gas-phase simulations, *Atmos. Environ*., *30B*, 1939–1963, 1996.

Jacobson, M. Z., Development and application of a new air pollution modeling system. Part III: Aerosol-phase simulations, *Atmos. Environ*., *31A*, 587–608, 1997.

Jacobson, M. Z., Studying the effects of aerosols on vertical photolysis rate coefficient and temperature profiles over an urban airshed, *J. Geophys. Res*., *103*, 10,593-10,604, 1998.

Jacobson, M. Z., Isolating nitrated and aromatic aerosols and nitrated aromatic gases as sources of ultraviolet light absorption, *J. Geophys. Res., 104*, 3527-3542, 1999.

Jacobson, M. Z., A physically-based treatment of elemental carbon optics: Implications for global direct forcing of aerosols, *Geophys. Res. Lett., 27*, 217-220, 2000.

Jacobson, M. Z., Strong radiative heating due to the mixing state of black carbon in atmospheric aerosols, *Nature, 409*, 695-697, 2001a.

Jacobson, M. Z., GATOR-GCMM: A global through urban scale air pollution and weather forecast model. 1. Model design and treatment of subgrid soil, vegetation, roads, rooftops, water, sea ice, and snow, *J. Geophys. Res., 106*, 5385-5401, 2001b.

Jacobson, M. Z., and G. M. Masters, Exploiting wind versus coal, *Science, 293*, 1438-1438, 2001.

Jacobson, M. Z., Control of fossil-fuel particulate black carbon plus organic matter, possibly the most effective method of slowing global warming, *J. Geophys. Res., 107* (D19), 4410, doi:10.1029/2001JD001376, 2002.

Jacobson, M. Z., The short-term cooling but long-term global warming due to biomass burning, *J. Clim., 17* (15), 2909-2926, 2004.

Jacobson, M. Z., J. H. Seinfeld, G. R. Carmichael, and D.G. Streets, The effect on photochemical smog of converting the U.S. fleet of gasoline vehicles to modern diesel vehicles, *Geophys. Res. Lett., 31,* L02116, doi:10.1029/2003GL018448, 2004.

Jacobson, M.Z., Studying ocean acidification with conservative, stable numerical schemes for nonequilibrium air-ocean exchange and ocean equilibrium chemistry, *J. Geophys. Res., 110,* D07302, doi:10.1029/2004JD005220, 2005a.

Jacobson, M.Z., *Fundamentals of Atmospheric Modeling, Second Edition*, Cambridge University Press, New York, 813 pp., 2005b.

Jacobson, M.Z., *W.G. Colella*, and D.M. Golden, Cleaning the air and improving health with hydrogen fuel cell vehicles, *Science*, *308*, 1901-1905, 2005.

Jacobson, M.Z., Effects of ethanol (E85) versus gasoline vehicles on cancer and mortality in the United States, *Environ. Sci. Technol*., *41* (11), 4150-4157, doi:10.1021/es062085v, 2007**.**

Jacobson, M.Z., Y.J. Kaufmann, Y. Rudich, Examining feedbacks of aerosols to urban climate with a model that treats 3-D clouds with aerosol inclusions, *J. Geophys. Res*., 112, D24205, doi:10.1029/2007JD008922, 2007

Jacobson, M.Z, On the causal link between carbon dioxide and air pollution mortality, *Geophysical Research Letters*, *35*, L03809, doi:10.1029/2007GL031101, 2008a**.**

Jacobson, M.Z., Effects of wind-powered hydrogen fuel cell vehicles on stratospheric ozone and global climate, *Geophys. Res. Lett*., 35, L19803, doi:10.1029/2008GL035102, 2008b.

Jacobson, M.Z., Review of solutions to global warming, air pollution, and energy security, *Energy & Environmental Science*, 2, 148-173, doi:10.1039/b809990c, 2009.

Jacobson, M.Z., and M.A. Delucchi, A path to sustainable energy by 2030, *Scientific American*, November 2009.

Jacobson, M.Z., Short-term effects of controlling fossil-fuel soot, biofuel soot and gases, and methane on climate, Arctic ice, and air pollution health, *J. Geophys. Res., 115*, D14209, doi:10.1029/2009JD013795, 2010a.

Jacobson, M.Z., The enhancement of local air pollution by urban CO_2 domes, *Environ. Sci. Technol., 44*, 2497-2502, doi:10.1021/es903018m, 2010b.

Jacobson, M.Z., and M.A. Delucchi, Providing all global energy with wind, water, and solar power, Part I: Technologies, energy resources, quantities and areas of infrastructure, and materials, *Energy Policy*, 39, 1154-1169, doi:10.1016/j.enpol.2010.11.040, 2011.

Jacobson, M. Z., *Air Pollution and Global Warming: History, Science, and Solutions*, Second Edition, Cambridge University Press, Cambridge, 375 pp., 2012a.

Jacobson, M.Z., Investigating cloud absorption effects: Global absorption properties of black carbon, tar balls, and soil dust in clouds and aerosols, *J. Geophys. Res*., *117*, D06205, doi:10.1029/2011JD017218, 2012b.

Jacobson, M.Z., and C.L. Archer, Saturation wind power potential and its implications for wind energy, *Proc. Nat. Acad. Sci*., *109*, 15,679-15,684, doi:10.1073/pnas.1208993109, 2012.

Jacobson, M.Z., and J.E. Ten Hoeve, Effects of urban surfaces and white roofs on global and regional climate, *J. Climate*, *25*, 1028-1044, doi:10.1175/JCLI-D-11-00032.1, 2012.

Jacobson, M.Z., R.W. Howarth, M.A. Delucchi, S.R. Scobies, J.M. Barth, M.J. Dvorak, M. Klevze, H. Katkhuda, B. Miranda, N.A. Chowdhury, R. Jones, L. Plano, and A.R. Ingraffea, Examining the feasibility of converting New York State's all-purpose energy infrastructure to one using wind, water, and sunlight, *Energy Policy*, 57, 585-601, 2013.

Jacobson, M.Z., Effects of biomass burning on climate, accounting for heat and moisture fluxes, black and brown carbon, and cloud absorption effects, *J. Geophys. Res*., *119*, 8980-9002, doi:10.1002/2014JD021861, 2014.

Jacobson, M.Z., C.L. Archer, and W. Kempton, Taming hurricanes with arrays of offshore wind turbines, *Nature Climate Change*, *4*, 195-200, doi: 10.1038/NCLIMATE2120, 2014a.

Jacobson, M.Z., M.A. Delucchi, A.R. Ingraffea, R.W. Howarth, G. Bazouin, B. Bridgeland, K. Burkhart, M. Chang, N. Chowdhury, R. Cook, G. Escher, M. Galka, L. Han, C. Heavey, A. Hernandez, D.F. Jacobson, D.S. Jacobson, B. Miranda, G. Novotny, M. Pellat, P. Quach, A. Romano, D. Stewart, L. Vogel, S. Wang, H. Wang, L. Willman, T. Yeskoo, A roadmap for repowering California for all purposes with wind, water, and sunlight, *Energy, 73,* 875-889, doi:10.1016/j.energy.2014.06.099, 2014b.

Jacobson, M.Z., 100% WWS plans for countries and states, United Nations Foundation Earth to Paris Social Good Event, UNFCC, Petit Palais, Paris, France, December 7, 2015, http://livestream.com/unfoundation/earthtoparisENG/videos/106549410 (accessed February 6, 2019).

Jacobson, M.Z., M.A. Delucchi, G. Bazouin, Z.A.F. Bauer, C.C. Heavey, E. Fisher, S. B. Morris, D.J.Y. Piekutowski, T.A. Vencill, T.W. Yeskoo, 100 percent clean and renewable wind, water, sunlight (WWS) all-sector energy roadmaps for the 50 United States, *Energy and Environmental Sciences*, *8*, 2093-2117, doi:10.1039/C5EE01283J, 2015a.

Jacobson, M.Z., M.A. Delucchi, M.A. Cameron, and B.A. Frew, A low-cost solution to the grid reliability problem with 100 percent penetration of intermittent wind, water, and solar for all purposes, *Proc. Nat. Acad. Sci*., *112* (*49*), 15,060-15,065 doi: 10.1073/pnas.1510028112, 2015b.

Jacobson, M.Z., M.A. Delucchi, G. Bazouin, M.J. Dvorak, R. Arghandeh, Z. A.F. Bauer, A. Cotte, G.M.T.H. de Moor, E.G. Goldner, C. Heier, R.T. Holmes, S.A. Hughes, L. Jin, M. Kapadia, C. Menon, S.A. Mullendore, E.M. Paris, G.A. Provost, A.R. Romano, C. Srivastava, T.A. Vencill, N.S. Whitney, and T.W. Yeskoo, A 100 percent wind, water, sunlight (WWS) all-sector energy plan for Washington State, *Renewable Energy*, *86*, 75-88 2016.

Jacobson, M.Z., M.A. Delucchi, Z.A.F. Bauer, S.C. Goodman, W.E. Chapman, M.A. Cameron, Alphabetical: C. Bozonnat, L. Chobadi, H.A. Clonts, P. Enevoldsen, J.R. Erwin, S.N. Fobi, O.K. Goldstrom, E.M. Hennessy, J. Liu, J. Lo, C.B. Meyer, S.B. Morris, K.R. Moy, P.L. O'Neill, I. Petkov, S. Redfern, R. Schucker, M.A. Sontag, J. Wang, E. Weiner, A.S. Yachanin, 100 percent clean and renewable wind, water, and sunlight (WWS) all-sector energy roadmaps for 139 countries of the world, *Joule, 1*, 108-121, doi:10.1016/j.joule.2017.07.005, 2017.

Jacobson, M.Z., M.A. Delucchi, M.A. Cameron, and B.V, Mathiesen, Matching demand with supply at low cost among 139 countries within 20 world regions with 100 percent intermittent wind, water, and sunlight (WWS) for all purposes, *Renewable Energy*, 123, 236-248, 2018a.

Jacobson, M.Z., M.A. Cameron, E.M. Hennessy, I. Petkov, C.B. Meyer, T.K. Gambhir, A.T. Maki, K. Pfleeger, H. Clonts, A.L. McEvoy, M.L. Miccioli, A.-K. von Krauland, R.W. Fang, and M.A. Delucchi, 100 percent clean, and renewable wind, water, and sunlight (WWS) all-sector energy roadmaps for 53 towns and cities in North America, *Sustainable Cities and Society*, *42*, 22-37, doi:10.1016/j.scs.2018.06.031, 2018b.

Jacobson, M.Z., V. Jadhav, World estimates of PV optimal tilt angles and ratios of sunlight incident upon tilted and tracked PV panels relative to horizontal panels, *Solar Energy*, 169, 55-66, 2018.

Jacobson, M.Z., The health and climate impacts of carbon capture and direct air capture, *Energy and Environmental Sciences*, *12*, 3567-3574, doi:10.1039/C9EE02709B, 2019.

Jacobson, M.Z., M.A. Delucchi, M.A. Cameron, S.J. Coughlin, C. Hay, I.P. Manogaran, Y. Shu, and A.-K. von Krauland, Impacts of Green-New-Deal energy plans on grid stability, costs, jobs, health, and climate in 143 countries, *One Earth*, *1, 449-463*, doi:10.1016/j.oneear.2019.12.003, 2019.

Jepsen, K., Ramboll Oil and Gas Operations Team (personal communications), 2018.

Johnson, G., When radiation isn't the real risk, 2015, https://www.nytimes.com/2015/09/22/science/when-radiation-isnt-the-real-risk.html (accessed December 8, 2018).

Jiang, Q., J.D. Doyle, T. Haack, M.J. Dvorak, *C.L. Archer*, and M.Z. Jacobson, Exploring wind energy potential off the California coast, *Geophys. Res. Lett*., 35, L20819, doi:10.1029/2008GL034674, 2008.

Kadiyala, A., R. Kommalapati, and Z. Huque, Evaluation of the lifecycle greenhouse gas emissions from different biomass feedstock electricity generation systems, *Sustainability, 8,* 1181-1192, 2016.

Kaldelis, J.K., and D. Apostolou, Life cycle energy and carbon footprint of offshore wind energy. Comparison with onshore counterpart, *Renewable Energy, 108*, 72-84, 2017.

Kahn, E., The reliability of distributed wind generators, *Electric Power Systems*, *2*, 1-14, 1979.

Kane, M., CATL breaks into 300+ Wh/kg energy density on battery cell level, 2019, https://insideevs.com/news/343690/catl-breaks-into-300-wh-kg-energy-density-on-battery-cell-level/ (accessed July 17, 2019).

Karam, P.A., How do fast breeder reactors differ from regular nuclear power plants, *Scientific American*, October 2006.

Katalenich, S.M., and M.Z. Jacobson, Toward battery electric and hydrogen fuel cell land, air, and sea military missions, in review, 2019.

Kempton, W., and J. Tomic, Vehicle-to-Grid Power Fundamentals: Calculating Capacity and Net Revenue, *J. Power Sources, 144*, 268-279, 2005a.

Kempton, W., and J. Tomic, Vehicle-to-grid power implementation: From stabilizing the grid to supporting large-scale renewable energy, *J. Power Sources, 144*, 280-294, 2005b.

Kempton, W., C.L. Archer, A. Dhanju, R.W. Garvine, and M.Z. Jacobson, Large CO_2 reductions via offshore wind power matched to inherent storage in energy end-uses, *Geophys. Res. Lett*., 34, L02817, doi:10.1029/2006GL028016, 2007.

Keith, D.W., G. Holmes, D. St. Angelo, and K. Heidel, A process for capturing CO_2 from the atmosphere, *Joule, 2*, 1573-1594, 2018.

Kirby, B.J., Frequency regulation basics and trends, ORNL/TM-2004/291, 2004, http://www.consultkirby.com/files/TM2004-291_Frequency_Regulation_Basics_and_Trends.pdf (accessed January 28, 2019).

Ko, N., M. Lorenz, R. Horn, H. Krieg, and M. Baumann, Sustainability assessment of concentrated solar power (CSP) tower plants – Integrating LCA, LCC, and LCWE in one framework, *Procedia CIRP 69*, 395-400, 2018.

Koomey, J., and N. E. Hultman, A reactor-level analysis of busbar costs for U.S. nuclear plants, 1970-2005, *Energy Policy 35*, 5630-5642, 2007.

Kougias, I., K. Bodis, A. Jager-Waldau, M. Moner-Girona, F. Monforti-Ferrario, H. Ossenbrink, and S. Szabo, The potential of water infrastructure to accommodate solar PV systems in Mediterranean islands, *Solar Energy, 136*, 174-182, doi:10.1016/j.solener.2016.07.003, 2016.

Krewski, D., M. Jerrett, R.T. Burnett, R. Ma, E. Hughes, Y. Shi, M.C. Turner, C. Arden Pope III, G. Thurston, E.E. Calle, and M.J. Thun, Extended follow-up and spatial analysis of the American Cancer Society study linking particulate air pollution and mortality, Health Effects Institute, Report No. 140, 2009.

Kuphaldt, T., What is alternating current (AC), 2019, https://www.allaboutcircuits.com/textbook/alternating-current/chpt-1/what-is-alternating-current-ac/ (accessed March 31, 2019)

Lackner, K.S., H.-J. Ziock, and P. Grimes, Carbon dioxide extraction from air: Is it an option? Report LA-UR-99-583, Los Alamos National Laboratory, 1999.

Lagarde, F., G. Pershagen, G. Akerblom, O. Axelson, U. Baverstam, L. Damber, A. Enflo, M. Svartengren, and G. A. Swedjemark, Residential radon and lung cancer in Sweden: risk analysis accounting for random error in the exposure assessment, *Health Physics*, *72*, 269-276, 1997.

Lazard, Lazard's levelized cost of energy analysis – version 12.0, 2018, https://www.lazard.com/media/450784/lazards-levelized-cost-of-energy-version-120-vfinal.pdf (accessed January 16, 2019).

Lenzen, M., Life cycle energy and greenhouse gas emissions of nuclear energy: A review, *Energy Conversion & Management*, *49*, 2178-2199, 2008.

Le Quere, C. et al., Global carbon budget 2014, *Earth Syst. Sci. Data, 7*, 47-85, 2015.

Lee, K.K., M.R. Miller, and A.S.V. Shah, Air pollution and stroke, J. Stroke, 20, 2-11, 2018.

Letterman, D., *The Late Show With David Letterman*, New York City, October 9, 2013, https://www.youtube.com/watch?v=AqIu2J3vRJc (accessed February 6, 2019).

Li, X., K.J. Chalvatzis, and D. Pappas, China's electricity emission intensity in 2020-an analysis at provincial level, *Energy Procedia, 142*, 2779-2785, 2017.

Liou, K.N., *An Introduction to Atmospheric Radiation*, Academic Press, Amsterdam, 2002.

Liu, H., G.B. Andresen, and M. Greiner, Cost-optimal design of a simplified highly renewable Chinese network, *Energy, 147*, 534-546, 2018.

Lu, B., A. Blakers, and M. Stocks, 90-100% renewable electricity for the South West Interconnected System of Western Australia, *Energy,122*, 663-674, 2017.

Lund, H., Large-scale integration of optimal combinations of PV, wind, and wave power into the electricity supply, *Renewable Energy, 31*, 503-515, 2006.

Lund, H., and B.V. Mathiesen, Energy system analysis of 100% renewable energy systems – The case of Denmark in years 2030 and 2050, *Energy, 34*, 524-531, 2009.

Lund, H., and B.V. Mathiesen, The role of carbon capture and storage in a future sustainable energy system, *Energy 44*, 469-476, 2012.

Macdonald-Smith, A., South Australia's big battery slashes $40m from grid control costs in first year, 2018, https://www.afr.com/business/energy/solar-energy/south-australias-big-battery-slashes-40m-from-grid-control-costs-in-first-year-20181205-h18ql1 (accessed January 25, 2019).

Manwell, J.F., J.G. McGowan, and A.L. Rogers, Wind energy explained – Theory, design, and application, John Wiley & Sons Ltd, p. 98, 2002.

Marine Energy, Global installed ocean energy power doubles in 2017, 2018 https://marineenergy.biz/2018/03/12/global-installed-ocean-energy-power-doubles-in-2017/ (accessed January 9, 2019).

Mason, I.G., S.C. Page, A.G. Williamson, A 100% renewable energy generation system for New Zealand utilizing hydro, wind, geothermal, and biomass resources, *Energy Policy 38*, 3973-3984, 2010.

Masters, G., *Renewable and Efficient Electric Power Systems*, 2nd Edition, Wiley, Hoboken, New Jersey, 712 pp., 2013.

Mathiesen, B.V., H. Lund, and K. Karlsson, 100% renewable energy systems, climate mitigation, and economic growth, *Applied Energy, 88*, 488-501, 2011.

Mathiesen, B.V., H. Lund, D. Connolly, H. Wenzel, P.Z. Ostergaard, B. Moller, S. Nielsen, I. Ridjan, P. Karnoe, K. Sperling, F.K. Hvelplund, Smart energy systems for coherent 100% renewable energy and transport solutions, *Applied Energy, 145*, 139-154, 2015.

Matthews, H.D., N.P. Gillett, P.A. Stott, and K. Zickfeld, The proportionality of global warming to cumulative carbon emissions, *Nature*, *459*, 829-832, 2009.

Matthews, H.D., *Montreal's emissions targets for 1.5 ^{o}C and 2 ^{o}C global warming*, 2016, http://ocpm.qc.ca/sites/ocpm.qc.ca/files/pdf/P80/7.2.19_damon_matthews.pdf (accessed January 13, 2018).

McFadyen, S., Three phase power simplified, 2012, https://myelectrical.com/notes/entryid/172/three-phase-power-simplified (accessed April 3, 2019).

Meador W. E. and W.R. Weaver, Two-stream approximations to radiative transfer in planetary atmospheres: A unified description of existing methods and a new improvement, *J. Atmos. Sci. 37*, 630-43, 1980.

Meinshausen, M. *et al*. Greenhouse-gas emission targets for limiting global warming to 2°C, *Nature* 458, 1158–1162, 2009.

Meyer, S., V. Franco, A. Lekov, L. Thompson, and A. Sturges, Do heat pump clothes dryers makes sense for the U.S. market, ACEEE Summer Study on Energy Efficiency in Buildings, 9-240- to 9-251, 2010, https://aceee.org/files/proceedings/2010/data/papers/2224.pdf (accessed October 29, 2019).

Miceli, F., Offshore wind turbines foundation types, 2012, http://www.windfarmbop.com/offshore-wind-turbines-foundation-types/ (accessed April 4, 2019).

MIT (Massachusetts Institute of Technology), *The Future of Natural Gas*, 287 pp., 2011, https://energy.mit.edu/wp-content/uploads/2011/06/MITEI-The-Future-of-Natural-Gas.pdf (accessed December 2, 2018).

Monitoring Analytics, Quarterly state of the market report for PJM: January through June, 2015, http://www.monitoringanalytics.com/reports/PJM_State_of_the_Market/2015/2015q2-som-pjm-sec5.pdf (accessed January 19, 2019).

Moore, M.A., A.E. Boardman, A.R. Vining, D.L. Weimer, and D.H. Greenberg, Just give me a number! Practical values for the social discount rate, *J. Policy Anal. Management, 23*, 789-812, 2004.

Moore, F.C. D.B. Diaz, Temperature impacts on economic growth warrant stringent mitigation policy, *Nature Climate Change, 5,* 127-131, 2015.

Morris, C., French nuclear power history – the unknown story, 2015, https://energytransition.org/2015/03/french-nuclear-power-history/ (accessed June 16, 2019).

Myhre, G., D. Shindell, F.-M. Breon, W. Collins, J. Fuglestvedt, J. Huang, D. Koch, J.F. Lamarque, D. Lee, B. Mendoza, T. Nakajima, A. Robock, G. Stephens, T. Takemura, and H. Zhang, *Anthropogenic and Natural Radiative Forcing*. In *Climate Change 2013: The Physical Science Basis. Contribution of Working Group I to the Fifth Assessment Report of the Intergovernmental Panel on Climate Change*. Stocker, T.F., D. Qin, G.-K. Plattner, M. Tignor, S.K. Allen, J. Boschung, A. Nauels, Y. Xia, V. Bex, and P.M. Midgley (eds.). Cambridge University Press, Cambridge, United Kingdom and New York, Ny, USA, 2013.

NACAG (Nitrac Acid Climate Action Group), Nitrous oxide emissions from nitric acid production, 2014, http://www.nitricacidaction.org/about/nitrous-oxide-emissions-from-nitric-acid-production/ (accessed December 1, 2018).

Nautical Almanac Office (NAO) and Her Majesty's Nautical Almanac Office, *Astronomical Almanac*. U. S. Government Printing Office, Washington, DC, 1993.

NASA (National Aeronautics and Space Administration), GISS surface temperature analysis (GISTEMP), 2018 https://data.giss.nasa.gov/gistemp/maps/ (accessed November 30, 2018).

NCEE (National Center for Environmental Economics), *Guidelines for Preparing Economic Analyses* (U.S. Environmental Protection Agency), 2014.

Neftel, A., H. Friedli, E. Moor, H. Lötscher, H. Oeschger, U. Siegenthaler, and B. Stauffer, Historical CO_2 record from the Siple Station ice core. In Trends: A Compendium of Data on Global Change, 1994. Carbon Dioxide Information Analysis Center, Oak Ridge National Laboratory, U.S. Department of Energy, Oak Ridge, Tenn., U.S.A.

Neocarbon Energy, Future energy system, http://neocarbonenergy.fi/internetofenergy/, 2016 (accessed December 6, 2016).

New York Times, Text of President Bush's remarks on global climate, 2001, https://www.nytimes.com/2001/06/11/world/text-of-president-bushs-remarks-on-global-climate.html (accessed February 2, 2019).
Ni, J., Carbon storage in grasslands of China, *J. Arid Environments, 50*, 205-218, 2002.
Nithyanandam K, and R. Pitchumani, Cost and performance analysis of concentrating solar power systems with integrated latent thermal energy storage*, Energy* 64: 793-810, 2014.
Nonbol, E., Load-following capabilities of nuclear power plants, Technical University of Denmark, 2013, http://orbit.dtu.dk/files/64426246/Load_following_capabilities.pdf (accessed November 22, 2018).
NRC (U.S. National Research Council), Real prospects for energy efficiency in the United States, National Academies Press, p. 251, https://www.nap.edu/read/12621/chapter/6#251, 2010 (accessed February 2, 2019).
NREL (National Renewable Energy Laboratory), *Jobs and Economic Development Impact Models (JEDI)*, 2017, https://www.nrel.gov/analysis/jedi (accessed January 17, 2019).
NREL (National Renewable Energy Laboratory), PV Watts Calculator, 2018, http://pvwatts.nrel.gov (accessed December 25, 2018).
NWCC (National Wind Coordinating Collaborative), Wind turbine interactions with birds, bats, and their habitats, 2010, https://www1.eere.energy.gov/wind/pdfs/birds_and_bats_fact_sheet.pdf (accessed January 4, 2018).
Oil and gas, Threat map, 2018, https://oilandgasthreatmap.com/threat-map/ (accessed December 3, 2018).
O'Malley, M., A jobs agenda for our renewable energy future, 2015, http://www.p2016.org/omalley/omalley070215climate.html (accessed February 7, 2019).
OMB (U.S. Office of Management and Budget), Circular A-4, Regulatory Analysis, the White House, Washington, D. C., September 17, 2003, https://www.whitehouse.gov/sites/whitehouse.gov/files/omb/circulars/A4/a-4.pdf (accessed January 16, 2019).
Orsted, New survey shows strong global support for green energy, November 13, 2017, https://orsted.com/en/Barometer (accessed February 7, 2019).
Ostro, B.D., H. Tran, and J.I. Levy, The health benefits of reduced tropospheric ozone in California*, J. Air & Waste Manage. Assoc., 56*, 1007-1021, 2006.
Pavel, C.C., R. Lacal-Arantegui, A. Marmier, D. Schuler, E. Tzimas, M. Buchert, W. Jenseit, and D. Blagoeva, Substitution strategies for reducing the use of rare earths in wind turbines, Resources Policy, 52, 349-357, 2017.
Pires, O., X. Munduate, O. Ceyhan, M Jacobs, and H. Snel, Analysis of high Reynolds numbers effects on a wind turbine airfoil using 2D wind tunnel test data, *J. Physics: Conference Series 753*, 022047, 2016.
Polpong, P. and S. Bovornkitti, Indoor radon, *Journal of the Medical Association of Thailand*, 81, 47-57, 1998.
Pope, C.A. III, R.T. Burnett, M.J. Thun, E.E. Calle, D. Krewski, K. Ito, and G.D. Thurston, Lung cancer, cardiopulmonary mortality, and long-term exposure to fine particulate air pollution, *JAMA, 287*, 1132-1141, 2002.
Puiu, T., Solar and wind supply more than 10% of electricity in 18 U.S. states, ZME Science, 2018, https://www.zmescience.com/science/news-science/solar-wind-electricity-us-stated-04232/ (accessed March 25, 2019).
Rahi, O.P., A. Kumar, Economic analysis for refurbishment and uprating of hydropower plants, *Renewable Energy, 86*, 1197-1204, 2016.
Rahman, D., A.J. Morgan, Y. Xu, R. Gao, W. Yu, D.C. Hopkins, and I. Husain, Design methodology for a planarized high power density EV/HEV traction drive using SiC power modules, 2016 IEEE Energy Conversion Congress and Exhibition, Sept. 18-22, 2016, doi: 10.1109/ECCE.2016.7855018, https://ieeexplore.ieee.org/document/7855018/authors#authors (accessed March 2, 2019).
Ram, M., D. Bogdanov, A. Aghahosseini, A. Gulagi, A.S. Oyewo, M. Child, U. Caldera, K. Sadovskaia, J. Farfan, L.S.N.S. Barbosa, M. Fasihi, S. Khalili, B. Dalheimer, G. Gruber, T. Traber, F. De Caluwe, H.-J. Fell, and C. Breyer, Global energy system based on 100% renewable energy – Power, heat, transport, and desalination sectors, Lappeenranta University of Technology Research Reports 91, ISSN: 2243-3376, Lappeenranta, Berlin, 2019, http://energywatchgroup.org/wp-

content/uploads/EWG_LUT_100RE_All_Sectors_Global_Report_2019.pdf (accessed September 6, 2019).
Ramaiah, R., and K.S.S. Shekar, Solar thermal energy utilization for medium temperature industrial process heat applications, *IOP Conf. Ser.: Mater. Sci. Eng., 376*, 010235, 2018.
Ramana, M.V., "Nuclear power: Economic, safety, health, and environmental issues of near-term technologies," *Annu. Rev. Environ. Resour.*, *34*, 127-152, 2009.
Ramboll, World's largest thermal heat storage pit in Vojens, 2016, https://stateofgreen.com/en/partners/ramboll/solutions/world-largest-thermal-pit-storage-in-vojens/ https://ramboll.com/projects/re/south-jutland-stores-the-suns-heat-in-the-worlds-largest-pit-heat-storage (accessed November 25, 2018).
Rasmussen, M.G., G.B. Andresen, and M. Greiner, Storage and balancing synergies in a fully or highly renewable pan-European power system, *Energy Policy, 51*, 642-651, 2012.
RE100, The world's most influential companies committed to 100% renewable power, 2019, http://there100.org (accessed January 26, 2019).
Rehau, Underground thermal energy storage, 2011 http://www.igshpa.okstate.edu/membership/members_only/proceedings/2011/100611-1030-B-Christopher percent20Fox percent20- percent20Rehau percent20- percent20Underground percent20Thermal percent20Energy percent20Storage.pdf (accessed November 21, 2018).
REN21 (Renewable Energy Policy Network for the 21st Century), Renewables 2019 global status report, 2019, https://www.ren21.net/gsr-2019/, https://www.ren21.net/gsr-2019/tables/table_06/table_06/ (accessed July 27, 2019).
Renewables Now, Chile's Coquimbo region nears 100% renewables share in H1 2019, 2019, https://renewablesnow.com/news/chiles-coquimbo-region-nears-100-renewables-share-in-h1-2019-663136/ (accessed July 26, 2019).
Roberts, D., The train goes up, the train goes down: a simple way to store energy, Vox, 2016, https://www.vox.com/2016/4/28/11524958/energy-storage-rail (accessed April 10, 2019)
Roselund, C., Inertia, frequency regulation and the grid, PV Magazine, 2019, https://pv-magazine-usa.com/2019/03/01/inertia-frequency-regulation-and-the-grid/ (accessed March 2, 2019).
Ruffalo, M.A., M. Krapels, and M.Z. Jacobson A plan to power the world with wind, water, and sunlight, Talks at Google, Google, Inc., Mountain View, California, June 20, 2012a, http://www.youtube.com/watch?v=N_sLt5gNAQs (accessed February 5, 2019).
Ruffalo, M.Z., M.Z. Jacobson, M. Krapels, and video from J. Fox, Powering the world, U.S., and New York with wind, water, and sunlight, The Nantucket Project, Nantucket, Massachusetts, October 6, 2012b, http://vimeo.com/52038463 (accessed February 5, 2019).
Russell, L.M., C.D. Cappa, M.J. Kleeman, and M.Z. Jacobson, Characterizing the climate impacts of brown carbon, Final report to the California Air Resources Board Research Division, Project 13-330, November 30, 2018.
Sadiqa, A., A. Gulagi, and C. Breyer, Energy transition roadmap towards 100% renewable energy and role of storage technologies for Pakistan by 2050, *Energy, 147*, 518-533, 2018.
Sadovskaia, K., D. Bogdanov, S. Honkapuro, and C. Breyer, Power transmission and distribution loses – a model based on available empirical data and future trends for all countries globally, *Electrical Power and Energy Systems, 107*, 98-109, 2019.
Sanders, B., Combatting climate change to save the planet, 2016, https://berniesanders.com/people-before-polluters/ (Accessed February 7, 2019).
Sanders, B., and M. Jacobson, he American people, not big oil, must decide our climate future, The Guardian, April 29, 2017, https://www.theguardian.com/commentisfree/2017/apr/29/bernie-sanders-climate-change-big-oil (Accessed February 7, 2019).
Santin, I., M. Barbu, C. Pedret, and R. Vilanova, Control strategies for nitrous oxide emissions reduction on wastewater treatment plants operation, *Water Research, 125*, 466-477, 2017.
Sanz-Perez, E.S., C.R. Murdock, S.A. Didas, and C.W. Jones, Direct capture of CO_2 from ambient air, *Chemical Reviews, 116*, 11,840-11,876, 2016.
Schubel, P.J., and R.J. Crossley, Wind turbine blade design, *Energies, 5*, 3425-3449, 2012.

Scottmadden, Billion dollar Petra Nova coal carbon capture project a financial success but unclear if it can be replicated, 2017, https://www.scottmadden.com/insight/billion-dollar-petra-nova-coal-carbon-capture-project-financial-success-unclear-can-replicated/ (accessed December 3, 2018).

Searchinger, T., R. Heimlich, R.A. Houghton, F. Dong, A. Elobeid, J. Fabiosa, S. Tokgoz, D. Hayes, and T.-H. Yu, Use of U.S. cropland for biofuels increases greenhouse gases through emissions from land-use change, *Science, 319*, 1238-1240, 2008.

Senate (U.S. Senate), S.Res.632, 2016, https://www.congress.gov/bill/114th-congress/senate-resolution/632 (accessed February 7, 2019).

Senate (U.S. Senate), S.987 – 100 by '50 Act, 2017," https://www.congress.gov/bill/115th-congress/senate-bill/987/text?r=1 (accessed February 7, 2019).

Senate (U.S. Senate), S.Res.59 – A resolution recognizing the duty of the Federal Government to create a Green New Deal, 2019," https://www.congress.gov/bill/116th-congress/senate-resolution/59?q=%7B%22search%22%3A%5B%22green+new+deal%22%5D%7D&s=1&r=2 (accessed March 26, 2019).

Sibbitt B, D. McClenahan, R. Djebbar, J. Thornton, B. Wong, J. Carriere, and J. Kokko, The performance of a high solar fraction seasonal storage district heating system – five years of operation, *Energy Procedia,* 30, 856-865, 2012.

Sierra Club, 100% commitments in cities, counties, and states, 2019, https://www.sierraclub.org/ready-for-100/commitments (accessed January 26, 2019).

Sirnivas, S., W. Musial, B. Bailey, and M. Filippelli, Assessment of offshore wind system design, safety, and operation standards, NREL/TP-5000-60573, 2014.

Skone, T.J., Lifecycle greenhouse gas emissions: Natural gas and power production, 2015 EIA Energy Conference, Washington DC, June 15, 2015, https://www.eia.gov/conference/2015/pdf/presentations/skone.pdf (accessed December 2, 2018).

Smallwood, K.S., Comparing bird and bat fatality rate estimates among North American wind energy projects, *Wildlife Society Bulletin, 37*, 19-33, 2013.

Socaciu, L., Seasonal sensible thermal energy storage solutions, *Leonardo Electronic Journal of Practices and Technologies, 10*, 49-68, 2011.

Solutions Project, Our 100% Clean Energy Vision, 2019 http://www.thesolutionsproject.org/why-clean-energy/ (accessed February 5, 2019).

Sorensen, B., A plan is outlined to which solar and wind energy would supply Denmark's needs by the year 2050, *Science, 189*, 255-260, 1975.

Sorensen, B., Scenarios of greenhouse warming mitigation, *Energy Convers. Mgmt, 37*, 693-698, 1996.

Sorensen, P.,A., and T. Schmidt, Design and construction of large scale heat storages for district heating in Denmark, 14th Int. Conf. on Energy Storage, April 25-28, Adana, Turkey, 2018, http://planenergi.dk/wp-content/uploads/2018/05/Soerensen-and-Schmidt_Design-and-Construction-of-Large-Scale-Heat-Storages-12.03.2018-004.pdf (accessed November 25, 2018).

Sourcewatch, The footprint of coal, 2011, https://www.sourcewatch.org/index.php/The_footprint_of_coal (accessed December 3, 2018).

Sovacool, B.K., Valuing the greenhouse gas emissions from nuclear power: A critical survey, *Energy Policy*, *36*, 2940-2953, 2008.

Sovacool, B.K., Contextualizing avian mortality: A preliminary appraisal of bird and bat fatalities from wind, fossil-fuel, and nuclear electricity, *Energy Policy, 37*, 2241-2248, 2009.

Spakovsky, Z.S., Trends in thermal and propulsive efficiency, 2008, http://web.mit.edu/16.unified/www/FALL/thermodynamics/notes/node84.html (accessed March 27, 2019).

Spath, P.L., and M.K. Mann, Life cycle assessment of a natural gas combined-cycle power generation system, National Renewable Energy Lab, NREL/TP-570-27715, 2000, http://www.nrel.gov/docs/fy00osti/27715.pdf, Accessed April 24, 2011.

Spector, J., 'Cheaper than a peaker': NextEra inks massive wind+solar+storage deal in Oklahoma, 2019, https://www.greentechmedia.com/articles/read/nextera-inks-even-bigger-windsolarstorage-deal-with-oklahoma-cooperative#gs.s8lb02 (accessed July 26, 2019).

Stagner, J., Stanford University's "fourth-generation" district energy system, District Energy, Fourth Quarter, 2016,

https://sustainable.stanford.edu/sites/default/files/IDEA_Stagner_Stanford_fourth_Gen_DistrictEnergy.pdf (accessed November 27, 2018).
Stagner, J., Stanford Energy System Innovations, Efficiency and environmental comparisons. 2017, https://sustainable.stanford.edu/sites/default/files/documents/SESI-CHP-vs-SHP-_percent26-CHC.pdf, (accessed November 24, 2018).
Statistica, Number of retail fuel stations in California from 2009 to 2016, by type, 2017, https://www.statista.com/statistics/818462/california-fueling-stations-by-type/ (accessed December 3, 2018).
Steinke, F., P. Wolfrum, and C. Hoffmann, Grid vs. storage in a 100% renewable Europe, *Renewable Energy, 50*, 826-832, 2013.
Stevens, F., and L. DiCaprio, Interviews at Stanford University for *Before the Flood*, 2014, https://cee.stanford.edu/programs/atmosphere-energy-program (accessed February 7, 2019).
Stone, D., Ferrock basics, 2017, http://ironkast.com/wp-content/uploads/2017/11/Ferrock-basics.pdf (accessed November 20, 2018).
Stoutenburg, E.D., N. Jenkins, and M.Z. Jacobson, Power output variations of co-located offshore wind turbines and wave energy converters in California, *Renewable Energy*, *35*, 2781-2791, doi:10.1016/j.renene.2010.04.033, 2010.
Stoutenburg, E.K., and M.Z. Jacobson, Reducing offshore transmission requirements by combining offshore wind and wave farms, *IEEE Journal of Oceanic Engineering*, *36*, 552-561, doi:10.1109/JOE.2011.2167198, 2011.
Stoutenburg, E.D., N. Jenkins, and M.Z. Jacobson, Variability and uncertainty of wind power in the California electric power system, *Wind Energy*, *17*, 1411-1424, doi:10.1002/we.1640, 2014.
Strata, The footprint of energy: Land use of U.S. electricity production, 2017, https://www.strata.org/pdf/2017/footprints-full.pdf (accessed December 3, 2018).
Streets, D. G., K. Jiang, X. Hu, J. E. Sinton, X.-Q. Zhang, D. Xu, M. Z. Jacobson, and J. E. Hansen, Recent reductions in China's greenhouse gas emissions, *Science, 294*, 1835-1836, 2001.
Talebizadeh, P., M.A. Mehrabian, and M. Abdolzadeh, Determination of optimum slope angles of solar collectors based on new correlations, *Energy Sources Part A., 33*, 1567-1580, 2011.
Tans, P., and R.F. Keeling (2015) Trends in atmospheric carbon dioxide, http://www.esrl.noaa.gov/gmd/ccgg/trends/#mlo_full (accessed January 24, 2019).
Ten Hoeve, J.E., and M.Z. Jacobson, Worldwide health effects of the Fukushima Daiichi nuclear accident, *Energy and Environmental Sciences*, *5*, 8743-8757, 2012.
Teske, S., D. Giurco, T. Morris, K. Nagrath, F. Mey, C. Briggs, E. Dominish, N. Florin, T. Watari, B. McLellan, T. Pregger, T. Naegler, S. Simon, J. Pagenkopf, B. van den Adel, O. Deniz, S. Schmidt, M. Meinhausen, K. Dooley, and ed. J. Miller, Achieving the Paris Climate Agreement, 2019, https://oneearth.app.box.com/s/hctp4qlk34ygd0mw3yjdtctsymsdtaqs (accessed September 6, 2019).
Tomasini-Montenegro, C., E. Santoyo-Castelazo, H. Gujba, R.J. Romero, and E. Santoyo, Life cycle assessment of geothermal power generation technologies: An updated review, *Applied Thermal Engineering, 114*, 1119-1136, 2017.
Toon, O.B. and T.P. Ackerman, Algorithms for the calculation of scattering by stratified spheres, *Appl. Opt., 20*, 3657-60, 1981.
Toon O.B., C.P. McKay, and T.P. Ackerman, Rapid calculation of radiative heating rates and photodissociation rates in inhomogeneous multiple scattering atmospheres, *J. Geophys. Res., 94*, 16,287-301, 1989.
Uddin, K., T. Jackson, W.D. Widange, G. Chouchelamane, P.A. Jennings, and J. Marco, On the possibility of extending the lifetime of lithium-ion batteries through optimal V2G facilitated by an integrated vehicle and smart-grid system, *Energy, 133*, 710-722, 2017.
Union Gas, Chemical composition of natural gas, 2018, https://www.uniongas.com/about-us/about-natural-gas/chemical-composition-of-natural-gas (accessed December 5, 2018).
U.S. DOI (U.S. Department of the Interior), Reclamation: Managing water in the west; Hydroelectric power, 2005, https://www.usbr.gov/power/edu/pamphlet.pdf (accessed November 22, 2018).
U.S. EPA (U.S. Environmental Protection Agency), 2008 U.S. National Emissions Inventory (NEI), 2011, https://www.epa.gov/air-emissions-inventories/2008-national-emissions-inventory-nei-data (accessed December 2, 2018).

U.S. EPA, Revision under consideration for the 2018 GHGI: Abandoned wells, 2017, https://www.epa.gov/sites/production/files/2017-06/documents/6.22.17_ghgi_stakeholder_workshop_2018_ghgi_revision_-_abandoned_wells.pdf (accessed December 3, 2018).

USGS (U.S. Geological Survey), *Mineral Commodities Summaries 2011*, U.S. Government Printing Office, Washington, D. C., 2018, https://minerals.usgs.gov/minerals/pubs/mcs/2018/mcs2018.pdf (accessed January 18, 2019).

USGS (United States Geological Survey), Lithium Statistics and Information, 2018, https://minerals.usgs.gov/minerals/pubs/commodity/lithium/mcs-2018-lithi.pdf (accessed November 23, 2018).

Ussiri, D., and R. Lal, Global sources of nitrous oxide, In *Soil emission of nitrous oxide and its mitigation*, Springer, pp. 131-175, 2012.

Van den Bergh, J.C.J.M., and W.J.W. Botzen, A lower bound the social cost of carbon emissions, *Nature Climate Change, 4*, 253-258, 2014.

Van den Bergh, J.C.J.M., and W.J.W. Botzen, Monetary valuation of the social cost of CO2 emissions: A critical survey, *Ecological Economics, 114*, 33-468, 2015.

Vavrin, J. Power and energy considerations at forward operating bases (FOBs). United States Army Corps of Engineers, Engineer Research and Development Center, Construction Engineering Research Laboratory, 2010 http://www.dtic.mil/dtic/tr/fulltext/u2/a566876.pdf (accessed February 13, 2019).

Viking Heat Engines, Heat Booster, 2019, http://www.vikingheatengines.com/news/vikings-industrial-high-temperature-heat-pump-is-available-to-order (accessed January 13, 2019).

Vogl, V., M. Ahman, and L.J. Nilsson, Assessment of hydrogen direct reduction for fossil-free steelmaking, *J. Cleaner Production, 203*, 736-745, 2018.

WEC (World Energy Council), World energy resources: Marine Energy, 2016, https://www.worldenergy.org/wp-content/uploads/2017/03/WEResources_Marine_2016.pdf (accessed January 9, 2019).

Wank, J., M.A. Ruffalo, Z. Saldana, and M.Z. Jacobson, Tommy and the Professor, 2012, https://www.youtube.com/watch?v=AqTID6Wv_xk&feature=youtu.be (accessed July 25, 2019).

Werner, S., International review of district heating, *Energy, 15*, 617-631, 2017.

Wiencke, J., H. Lavelaine, P.-J. Panteix, C. Petijean, and C. Rapin, Electrolysis of iron in a molten oxide electrolyte, *J. Applied Electrochemistry, 48*, 115-126, 2018.

Wigley, T.M.L., Coal to gas: the influence of methane leakage, *Climatic Change, 108*, 601-608, 2011.

Winther, M., D. Balslev-Harder, S. Christensen, A. Prieme, B. Elberling, E. Crosson, and T. Blunier, Continuous measurements of nitrous oxide isotopomers during incubation experiments, *Biogeosciences, 15*, 767-780, 2018.

WHO (World Health Organization), 7 million premature deaths annually linked to air pollution, 2014, http://www.who.int/mediacentre/news/releases/2014/air-pollution/en/ (accessed July 26, 2019).

WHO (World Health Organization) Health statistics and information systems, 2017a, https://www.who.int/healthinfo/global_burden_disease/estimates/en/ (accessed July 26, 2019).

WHO (World Health Organization), Global health observatory data, 2017b, https://www.who.int/gho/phe/outdoor_air_pollution/en/ (accessed July 26, 2019).

WHO (World Health Organization), Mortality from environmental pollution, 2017c, http://apps.who.int/gho/data/node.sdg.3-9-data?lang=en (accessed July 26, 2019).

Wilkerson, J.T., M.Z. Jacobson, A. Malwitz, S. Balasubramanian, R. Wayson, G. Fleming, A.D. Naiman, and S.K. Lele, Analysis of emission data from global commercial aviation: 2004 and 2006, *Atmos. Chem. Phys., 10*, 6391-6408, 2010.

Winnefeld, C., T. Kadyk, B. Bensmann, U. Krewer, and R. Hanke-Rauschenback, Modelling and designing cryogenic hydrogen tanks for future aircraft applications, *Energies, 11*, 105, doi:10.3390/en11010105, 2018.

Wiser, R., M. Bolinger, G. Barbose, N. Darghouth, B. Hoen, A. Mills, J. Rand, D. Millstein, S. Jeong, K. Porter, N. Disanti, and F. Oteri, 2018 wind technologies market report, U.S. Department of Energy, 2019 http://eta-publications.lbl.gov/sites/default/files/wtmr_final_for_posting_8-9-19.pdf (accessed August 16, 2019).

Woodford, C., Lithium ion batteries, 2018, https://www.explainthatstuff.com/how-lithium-ion-batteries-work.html (accessed March 26, 2019).
World Bank, Agricultural and rural development, https://data.worldbank.org/indicator/ (2017) (accessed September 16, 2019).
World Bank, Electric power transmission and distribution losses (% of output), 2018, https://data.worldbank.org/indicator/EG.ELC.LOSS.ZS?end=2014&start=2009 (accessed January 1, 2019).
World Nuclear Association, World uranium mining production, 2019, http://www.world-nuclear.org/information-library/nuclear-fuel-cycle/mining-of-uranium/world-uranium-mining-production.aspx (accessed March 30, 2019).
World Nuclear News, Green light for next Darlington refurbishment, 2018, http://world-nuclear-news.org/Articles/Green-light-for-next-Darlington-refurbishment (accessed December 7, 2018).
Worldwatch Institute, Energy poverty remains a global challenge for the future, 2019, http://www.worldwatch.org/energy-poverty-remains-global-challenge-future (accessed February 13, 2019).
Zapata, S., M. Casteneda, M. Jiminez, A.J. Aristizabel, C.J. Franco, and I. Dyner, Long-term effects of 100% renewable generation on the Colombian power market, Sustainable Energy Technologies and Assessments, 30, 183-191, 2018.
Zhang, J., S. Chowdhury, and J. Zhang, Optimal preventative maintenance time windows for offshore wind farms subject to wake losses, AIAA 2012-5435, 2012.
Zhou, L., Y. Tian, S.B. Roy, C. Thorncroft, L.F. Bosart, and Y. Hu, Impacts of wind farms on land surface temperature, *Nature Climate Change 2*, 539-543, 2012.